

1 **Deposition and provenance of the Early Pleistocene Siliceous Member in**
2 **Westbury Cave, Somerset, England**

3

4 Neil F. Adams ^{a,b,*,1}, Ian Candy ^a, Danielle C. Schreve ^a, René W. Barendregt ^c

5

6 ^a Centre for Quaternary Research, Department of Geography, Royal Holloway

7 University of London, Egham, Surrey, TW20 0EX, UK

8 ^b Department of Earth Sciences, Royal Holloway University of London, Egham,

9 Surrey, TW20 0EX, UK

10 ^c Department of Geography, University of Lethbridge, Lethbridge, T1K 3M4, Canada

11

12 * Author for correspondence (e-mail: nfa10@leicester.ac.uk)

13

14 ¹ Present address: Centre for Palaeobiology Research, School of Geography,

15 Geology and the Environment, University of Leicester, Leicester, LE1 7RH, UK

16 **Abstract**

17 The Early Pleistocene is an important interval in the Quaternary period as a time not
18 only of climatic and environmental change, but also of key events in human
19 evolution. However, knowledge of this period in northwest Europe is hampered by
20 the limited extent of deposits of this age. Westbury Cave in the Mendip Hills of
21 Somerset preserves an understudied example of fossil-bearing Early Pleistocene
22 sediments, with rare potential to inform our understanding of British Early
23 Pleistocene stratigraphy and landscape evolution outside the East Anglian Crag
24 Basin. This study identifies the processes responsible for deposition of the Early
25 Pleistocene Siliceous Member in Westbury Cave, thereby aiding taphonomic and
26 palaeoenvironmental interpretations of associated fossil assemblages. New
27 excavations revealed over ten metres of Siliceous Member stratigraphy, dominated
28 by fine-grained silts/clays with interbedded sands and gravels, interpreted as being
29 deposited within a subterranean lake or flooded conduit with fluvial input. All
30 sediments sampled were reversely magnetised and are assigned to the Matuyama
31 Reversed Chron. Lithological analysis of gravel clasts revealed variable components
32 of durable non-local and non-durable local clasts. Gravels containing the latter are
33 interpreted as distal talus slope deposits, and those lacking non-durable lithologies
34 as stream or flood deposits. However, it remains unclear from available data whether
35 apparently non-local clasts were sourced from long distance or stem from a more
36 local, now denuded catchment. Siliceous Member bio- and magnetostratigraphy
37 suggest that deposition occurred late in the Early Pleistocene, a period otherwise
38 unrepresented in the UK.

39 **Keywords**

40 cave sedimentation; clast lithology; Early Pleistocene; palaeomagnetic dating;

41 Siliceous Member; Westbury Cave

42

43 **1. Introduction**

44 The Early Pleistocene is an important interval in the Quaternary period as a time not
45 only of climatic and environmental change, but also of key events in human evolution
46 (McClymont et al., 2013; Lordkipanidze et al., 2013). During the course of this
47 interval (ca. 2.58-0.78 Ma), the glacial cycles that characterise the Quaternary shift
48 from being dominated by a ~40-kyr cyclicity to a ~100-kyr cyclicity with the transition
49 between the two, beginning at ca. 1.2 Ma, being known as the mid-Pleistocene
50 revolution or MPR (Fig. 1; Lisiecki and Raymo, 2005; McClymont et al., 2013;
51 Kender et al., 2018). In the terrestrial environments of regions such as western and
52 central Europe, this shift means that extensive lowland glaciation and major falls in
53 eustatic sea level were restricted to the Middle and Late Pleistocene, with the
54 magnitude of Early Pleistocene glacial cycles being insufficient to generate the
55 prolonged and intense cooling necessary to form these environments (Rose, 2009;
56 Lee et al., 2018). Against this complex pattern of climate change, a number of major
57 early human dispersals occurred, including the earliest appearance of hominins
58 outside of Africa (Gabunia et al., 2000; Dennell and Roebroeks, 2005; Zhu et al.,
59 2008), the earliest occupation of the Mediterranean basin (Arzarello et al., 2012;
60 Toro-Moyano et al., 2013; Michel et al., 2017) and the first known hominin
61 occurrences in Europe north of the Alps (Parfitt et al., 2010; Ashton et al., 2014).

62

63 Our understanding of this complex and important time interval is restricted by the
64 scarcity of detailed palaeoenvironmental archives that span the Early Pleistocene.
65 The antiquity of this period means that progressive erosion and denudation have
66 removed large portions of the deposits of this age, making the study of the Early
67 Pleistocene problematic in many regions of the world; a good example of this is the
68 record from the British Isles (Gibbard et al., 1991; Jones and Keen, 1993; Rose,
69 2009; Lee et al., 2018) as well as from nearby continental Europe. Early Pleistocene
70 palaeoenvironments, palaeogeography and palaeohydrology in Britain are best
71 represented in terrestrial river terraces (the Kesgrave and Bytham Catchments
72 Subgroups of the Dunwich Group) across central and southeast England (e.g.,
73 Bridgland, 1988; Gibbard, 1988; Whiteman, 1992; Rose, 1994; Rose et al., 1999;
74 Westaway et al., 2002; Westaway, 2009) and, more particularly, in the extensive
75 shallow marine-estuarine Crag Group sediments of the East Anglian Crag Basin, the
76 western extension of the southern North Sea Basin (e.g., West, 1962, 1980; Mathers
77 and Zalasiewicz, 1988; Funnell, 1995, 1996; Rose et al., 2001, 2002; Rose, 2009;
78 Parfitt et al., 2010; Preece and Parfitt, 2012; Ashton et al., 2014). The sediments of
79 the Crag Basin have also yielded the only purported Early Pleistocene hominin
80 records in Britain (Parfitt et al., 2010; Ashton et al., 2014; but see Westaway, 2011
81 and Preece and Parfitt, 2012 for discussion of the disputed age of these records).
82
83 Nevertheless, the information that the Crag Basin deposits provide is limited for three
84 reasons. Firstly, the spatial extent of the Crag Group deposits is confined to a
85 restricted area of East Anglia, consequently, the sequences in question provide
86 minimal information for the rest of the British Isles (Jones and Keen, 1993).
87 Secondly, the Early Pleistocene shallow marine Crag sediments extend to no

88 younger than 1.8 Ma (Red and Norwich Crag Formations) with no further well-dated
89 sedimentation occurring in the region until at least 0.78 Ma (Cromer Forest Bed
90 Formation, CFBF; Fig. 1), a sedimentary hiatus of more than 1 Ma that covers over
91 half of the Early Pleistocene (Gibbard et al., 1991, but see also Rose et al., 2001).
92 One possible exception occurs at the site of Happisburgh 3, where the Hill House
93 Member of the CFBF has been suggested to date to the late Early Pleistocene (Fig.
94 1; Parfitt et al., 2010, Gibbard, 2012; but see Westaway, 2011). The hiatus means
95 that the stratigraphy, environments and ecosystems of Britain during the rest of the
96 Early Pleistocene are poorly understood. Finally, faunal assemblages from these
97 shallow marine-estuarine deposits unsurprisingly demonstrate a taphonomic bias
98 towards aquatic vertebrates (mostly fish) and invertebrates (largely marine
99 molluscs). Terrestrial fossils are therefore relatively rare components of these fossil
100 assemblages and represent occasional specimens transported down river estuaries
101 into the Crag Basin, thus reducing the information that can be gleaned about
102 terrestrial ecosystems at this time.

103

104 Sedimentary records of this age are extremely sparse in adjacent areas of
105 continental north-west Europe. The few examples of Early Pleistocene deposits in
106 northern France include the upper part of the estuarine/marine Formation de la
107 Baronnerie in the Pas-de-Calais (Sommé, 2013) and the highest terrace of the River
108 Somme (Ferme de Grâce at Montières, Terrace IX of Antoine, 1990) but neither
109 have yielded vertebrate fossils beyond a single stenonid horse tooth from the latter
110 (Auguste, 1995). The sediments of the Crag Basin can be partially correlated with
111 the better-established stratigraphical successions in the Netherlands and northern
112 Belgium (Kasse, 1990), which formed the eastern part of the North Sea Basin. The

113 Belgian and Dutch Early Pleistocene successions are characterised by a stacked
114 series of fluvial deposits laid down by the Rhine, Meuse and Scheldt rivers, with
115 climato-stratigraphical subdivision based largely on evidence for periglacial
116 conditions (e.g., Vandenberghe and Kasse, 1989) and pollen biostratigraphy (e.g.,
117 Zagwijn, 1957, 1985), supplemented by rich assemblages of plant macrofossils
118 (Reid and Reid, 1907), molluscs (e.g., Meijer, 1986), reptiles and amphibians (Villa
119 et al., 2018), and large and small mammals (summarised in van den Hoek Ostende,
120 2004). Although the Dutch sedimentary succession is thicker and more complete
121 than in Britain (Gibbard et al., 1991) (notwithstanding the presence of several
122 significant hiatuses), it nevertheless remains extremely difficult to correlate evidence
123 for local climatic change with the marine oxygen isotope record. The position of the
124 Crag Basin, near the western hinge line of the North Sea Basin, has further meant
125 that uplift and changing sea level have led to significant gaps in the East Anglian
126 sequence that are not apparent in the Dutch sequence (Preece and Parfitt, 2012).

127

128 Cave and fissure sites provide the only known Early Pleistocene terrestrial archives
129 with palaeoenvironmental data from regions of Britain outside East Anglia, but these
130 sites are few and have received little prior attention. Dove Holes Cave in Victory
131 Quarry, Derbyshire (Dawkins, 1903; Spencer and Melville, 1974), the Dewlish bone
132 fissure in Dorset (Fisher, 1877, 1888, 1905, 1913; Carreck 1955), and Westbury
133 Cave in Somerset (Bishop, 1982; Andrews et al., 1999) have all yielded limited Early
134 Pleistocene vertebrate assemblages. However, Dove Holes Cave, a narrow cave
135 system formed within the Carboniferous Bee Low Limestone Formation, has long
136 been emptied of sediment and destroyed by quarrying (see Anon., 1917) and the

137 Dewlish bone fissure, a sand- and gravel-filled fissure in the Cretaceous White Chalk
138 Subgroup, has not been re-located since original excavation over a century ago.
139
140 Westbury Quarry (grid ref.: ST 506 504; 51°14'59"N, 2°42'28"W), 1.5 km north of the
141 village of Westbury-sub-Mendip, lies on the southern flanks of the Mendip Hills in
142 Somerset, southwest England (Fig. 2). The Mendip Hills consist dominantly of
143 Palaeozoic rocks (Silurian-Carboniferous) that were uplifted and folded into anticlinal
144 pericline structures during the Variscan Orogeny in the late Carboniferous to early
145 Permian (Green and Welch, 1965; Fig. 3). These Palaeozoic strata were then
146 overstepped by Triassic-Jurassic, as well as recently identified Cretaceous, rocks
147 (Farrant et al., 2014; Fig. 3), represented by clear angular unconformities. It is in the
148 extensive Carboniferous limestones that large cave systems have developed (Ford
149 and Stanton, 1968). The well-preserved *in situ* Early Pleistocene cave deposits at
150 Westbury Quarry were discovered relatively recently, in 1969 (Heal, 1970), by
151 quarrying through the Carboniferous Clifton Down Limestone Formation (Fig. 2). The
152 Pleistocene sediments at the site can be divided into two main stratigraphical units
153 (Stanton, 1973; Bishop, 1974, 1982; Andrews et al., 1999): 1) the Early Pleistocene
154 "Siliceous Member" and 2) the early Middle Pleistocene "Calcareous Member". The
155 latter has received greater attention and is comprised of coarse limestone cave
156 breccias that contain a diverse vertebrate assemblage and several disputed early
157 human artefacts, which at the time of discovery, were thought to represent the
158 earliest hominin occupation of Britain (Bishop, 1975; Andrews et al., 1999; Cook,
159 1999). The Calcareous Member is underlain by sands and gravels of the Siliceous
160 Member that have consistently yielded fossils, albeit fewer than those of the
161 overlying unit (Bishop, 1982).

162

163 Of the three fossiliferous Early Pleistocene sites located outside East Anglia,
164 Westbury has the best potential to address current gaps in our knowledge, in that: 1)
165 it contains a long and well-stratified sequence of deposits that has yielded a diverse
166 range of fossiliferous material, and 2) on the basis of both bio- and
167 magnetostratigraphy, the Westbury deposits can be proven to be convincingly of
168 Early Pleistocene age but also younger than the Crag deposits of East Anglia
169 (Bishop, 1982, Yassi, 1983, Farrant, 1995, Gentry, 1999; Fig. 1). The Early
170 Pleistocene succession at Westbury, therefore, has the potential to provide important
171 information on a hitherto poorly understood part of the Quaternary of Britain.

172

173 Despite their importance, the Early Pleistocene sediments at Westbury have
174 received limited study since the 1970s, partly because of the limited exposure over
175 the last four decades and partly because of greater attention being paid to the
176 younger early Middle Pleistocene deposits at the same site. In particular, the nature
177 of the sedimentary processes that were responsible for the accumulation of these
178 deposits is poorly understood, despite being critical for the accurate taphonomic and
179 (bio)stratigraphical interpretation of the contained fossil assemblages. This paper
180 presents the first results from a recent re-investigation of the Early Pleistocene
181 sequence at Westbury and outlines the detailed sedimentology of the sequence,
182 using palaeomagnetic dating to demonstrate an unequivocal Early Pleistocene age,
183 before then constructing a depositional model for the accumulation of this record.
184 These results highlight the complexity of the Westbury sequence and will provide the
185 basis for ongoing analyses of the fossil assemblages and the geochronology of the

186 sediments, as well as contributing new details to our knowledge of the British
187 Quaternary stratigraphical record.

188

189 **2. Material and methods**

190 **2.1. Excavation and field sections**

191 An initial visit to Westbury Quarry in March 2014 revealed the current extent of
192 Pleistocene cave sediment exposures (see Supplementary Material Fig. S1). Six
193 faces (each ca. one metre in height) were cleaned back to expose in situ sediments
194 for description and sampling in June-July 2014 (S1a; Fig. 4). A second deeper
195 section was also dug several metres to the west of S1a in June-July 2014 to
196 exposed older Siliceous Member sediments (S2; Fig. 4). In December 2015, the top
197 of S1a was extended to the east to reveal the contact with the overlying early Middle
198 Pleistocene Calcareous Member (S1b; Fig. 4). In April 2016, S1a was also extended
199 to the west to connect with top of S2 (S1c; Fig. 4). A datum point at the top of S1a
200 (225 m AOD) was used to establish stratigraphical control and to determine the
201 depths from which clast lithological and other samples were taken.

202 The exposure and description of sediment faces followed the procedure of Jones et
203 al. (1999). Each face was drawn by identifying the main depositional units and then
204 adding finer detail of individual beds, with field determination of grain size, sediment
205 texture, and colour (using a Munsell colour chart). The faces were photographed
206 using a Nikon D5200 camera.

207

208 **2.2. Particle size analysis**

209 One sediment sample of ca. 500 grams was taken from each facies type for particle
210 size analysis (see Fig. 5 for sampling locations within each face). Particle size was

211 determined by a combination of wet- and dry-sieving for the >63 µm fraction,
212 following procedures in Gale and Hoare (1991). The <63 µm fraction was determined
213 with a Micromeritics SediGraph 5100 (Micromeritics Instrument Corporation,
214 Norcross, GA, USA), which uses X-rays to measure the size of dispersed particles
215 as they settle through a liquid (Stein, 1985), following the method established by
216 Coakley and Syvitski (1991). The two datasets were combined to generate a particle
217 size distribution. Particle size statistics were generated using GRADISTAT, version
218 8.0 (Blott and Pye, 2001).

219

220 **2.3. Clast lithology**

221 Bulk sediment samples were taken from five coarse-grained units of S1a (F1U2,
222 F3U2/F4U1, and F5U3/F6U1). These bulk sediment samples were taken for clast
223 lithology analysis and to process for vertebrate fossils. The faunal assemblage
224 recovered during the excavations is currently under study and will be reported upon
225 separately. A minimum of 20 litres of sediment was extracted every 20 cm through
226 the coarse-grained units, although the volume of sediment extracted and sampling
227 frequency varied due to variation in fossil content and the extent of the deposits. Bulk
228 samples were wet-sieved through a 500 µm mesh, and residues were then graded
229 using a nested column of sieves (16, 8, 4, 2, 1, and 0.5 mm). Graded residues were
230 subsampled for clast lithology analysis, following the procedure of Bridgland (1986).
231 The lithology of the >16 mm and 8-16 mm fractions from coarse-grained units
232 (following procedures in Bridgland, 1986) was determined under a low-power
233 binocular microscope. Clasts were broken in some cases to observe fresh,
234 unweathered faces and hydrochloric acid was used to verify the identification of
235 carbonate limestone clasts (Bridgland, 1986).

236

237 **2.4 Palaeomagnetic dating**

238 Outcrop sampling was carried out by inserting polycarbonate plastic cylinders
239 horizontally into cleaned vertical faces excavated along the exposure. Cylinders
240 have a sharpened and tapered cutting edge, and internal raised splines on the base
241 and side which serve as orientation marks and prevent movement of sediment inside
242 the cylinder. Insertion azimuths of cylinders were measured using a magnetic
243 compass corrected for the magnetic declination at the sampling site. Samples were
244 generally selected from sorted, fine-grained sediments. Where fine-grained
245 sediments were not present, samples were taken from sorted coarser deposits
246 containing a sufficiently fine-grained matrix. Sediments containing pebbles were
247 avoided. In this manner, it was possible to sample all faces of the Siliceous Member
248 S1a section. Within each face, samples were collected in horizontal sequence, from
249 each of the subunits identified, typically from the base, middle and top. Sample
250 cylinders were sealed to prevent drying and oxidation, and stored in a magnetic
251 shield following field collection and between laboratory measurements.

252

253 To help constrain the age of the Siliceous Member sediments, palaeomagnetic
254 measurements were carried out on oriented samples (see Fig. 5 for sampling
255 locations) to ascertain polarity. Remanence measurements were carried out at the
256 Environmental Paleomagnetism Laboratory, University of Lethbridge, using a JR-6A
257 spinner magnetometer (AGICO, Brno, Czech Republic). We measured the natural
258 remanent magnetisation (NRM) of each of the 52 samples collected, and re-
259 measured the remanence after stepwise demagnetisation in alternating fields
260 (typically 5-12 steps ranging from 5 to 160 mT) using an ASC Scientific D-2000

261 alternating-field (AF) demagnetiser with three axis manual tumbler. Characteristic
262 remanent magnetisation (ChRM) directions were determined by principal component
263 analysis (PCA; Kirschvink, 1980) using at least three points on the demagnetisation
264 curve directed toward the origin, when plotted on an orthogonal projection. Only
265 points with a maximum angular standard deviation (MAD) $\leq 5^\circ$ were selected. Mean
266 remanence directions of sample groups were determined from PCA results of
267 individual samples. Overall means were calculated from all coherent individual
268 specimens, and for each of the five sampled faces. Remasoft version 3.0 (AGICO,
269 Brno, Czech Republic) palaeomagnetic data analysis software was used in these
270 calculations. Magnetic susceptibility (a measure of the bulk magnetite content) was
271 measured using a Sapphire Instruments (SI-2B) susceptibility meter.

272

273 **3. Results**

274 **3.1. Siliceous Member stratigraphy**

275 Over ten metres of Siliceous Member sediments were exposed during excavations.
276 The sequence is underlain by Carboniferous limestone bedrock (contact not seen)
277 and overlain by an erosive contact with the overlying Calcareous Member (Fig. 8).
278 The Siliceous Member comprises beds of sands, fines (silts and clays) and well-
279 rounded gravels (granular to pebble in grain size) with very rare cobbles and
280 boulders of angular limestone (Figs. 5-8). Lithofacies were identified and grouped
281 into facies associations that could be used to define a particular depositional
282 environment (see facies descriptions, abbreviations and associations in Table 1).
283 Units are referred to in the text by the face number followed by the unit number
284 within each face, e.g., F1U2 refers to the second unit seen in the first sediment face.

285

286 3.1.1. Facies Association A

287 This facies association forms the dominant sediment type in the succession, with
288 units of horizontally-bedded sands and fines. It is composed of two facies: (1) sand-
289 dominated beds (either massive or cross-bedded) with silt and clay drapes ('flaser-
290 like' structures – Sfl; Fig. 5) and (2) beds dominated by the fine component with thin
291 and discontinuous laminations (ca. 1 mm thick) or lenses (up to 5 cm thick) of
292 medium sand ('lenticular-like' bedding – Flt; Fig. 5). For the most part, the silt and
293 clay beds are green/grey in colour with evidence for iron remobilisation (iron pans
294 and sediment staining) being restricted to upper and lower contacts between these
295 beds and the coarser-grained sands and gravels. The relationship between these
296 facies is complex and often involves only subtle changes in the dominance of sand
297 over finer grain sizes, or vice versa. Where finer grain sizes dominate, the sand
298 occurs as discrete lenses or thin continuous interbedded sheets (e.g., F4U3 in Fig.
299 5d shows a dominance of sand lenses passing up into thinner sand sheets). In other
300 areas, the finer grain sizes form lenses within largely sandy units (e.g., F2U2 in Fig.
301 5b).

302

303 Facies association A is found at the base of S1a (F6U4) and is repeated many times
304 up-section (see Table 1 for units; Fig. 5). It is also found at the base of S1b (Fig. 6)
305 and at the top of S1c in F2U1 (Fig. 7), which links laterally to F5U1 of S1a. This
306 association also made up the majority of Section 2 (Fig. 8), which underlies Section
307 1. Bounding surfaces with other facies associations (e.g., facies associations B, C,
308 and D) are dominantly erosional contacts, where coarser units containing gravel-
309 sized particles have cut down into facies association A deposits.

310

311 The units of F3 in S1a dip steeply southeast (see Supplementary Material Fig. S2),
312 so the sediments of F4 are simply down-dip continuations of F3 units, but extend
313 stratigraphically deeper. There is a major unconformity in F3 and F4, shown by the
314 angular truncation of the horizontally bedded sands and silts of F3U3/F4U3 by the
315 inclined silts, sands and gravels of F3U2/F4U2 (Fig. 5).

316

317 **3.1.2. Facies Association B**

318 At the base of S1 there is a coarser-grained unit of stratified, steeply dipping ($>30^\circ$)
319 sands and gravels (Gs). The gravel components range up to pebble-size. This unit
320 shows evidence of iron remobilisation, having brown and red colourations and the
321 presence of thin iron pans. This association is found in units of F5-F6 of S1a (Fig. 5)
322 and F1-F2 of S1c (Fig. 7). This association is bounded by erosive contacts with
323 facies association A sediments above and below (Fig. 5e-f).

324

325 **3.1.3. Facies Association C**

326 Facies association C consists of beds of channelized coarse sand, granules and
327 pebbles (Gch; Table 1). Bedding within these coarse lenses is either horizontal or
328 trough-like in form. The coarser units all show evidence for iron remobilisation with
329 orange, brown and red colourations and the presence of thin iron pans.

330

331 In F4 and F3 of S1a, these coarse sediments have cut down into the finer-grained
332 deposits of facies association A (F4U2-3, F3U3), resulting in an erosive bounding
333 surface (Fig. 5).

334

335 **3.1.4. Facies Association D**

336 Facies association D consists of horizontal beds of coarse sand (Sfl), granules and
 337 pebbles (Gm). Bedding within these coarse lenses is either horizontal or trough-like
 338 in form. Within the coarser units, many of the beds are bounded by erosive
 339 unconformities above and below. These coarser units also show evidence of iron
 340 remobilisation and have thin iron pans. Within this facies association, sand beds are
 341 often thinly interbedded as lenses or sheets with the thicker gravels (e.g., F1U2 in
 342 S1a, Fig. 5a), but occasionally form beds of greater thickness (e.g., F1U2 in S1c,
 343 Fig. 7a)

344

345 These sediments occur higher in S1a (in F3 and F1) than other coarse grained
 346 facies associations and overlie deposits of facies association A (Fig. 5), with the
 347 lower contact cutting across the top of the underlying sands and fines. Deposits of
 348 facies association D are also found in F1U2 of S1b (Fig. 6), which laterally links to
 349 F1U2 of S1a, and in F1U3 and F1U2/F2U3 of S1c (Fig. 7). This facies association is
 350 also found in Section 2 between deposits of facies association A.

351

352 **3.1.5. Facies Association E**

353 Facies association E consists of a coarse (cobble/boulder) limestone breccia (Br),
 354 matching previous descriptions of the Calcareous Member (Fig. 6). In S1b, this
 355 breccia truncates and overlies the lateral equivalent of the upper most beds of facies
 356 associations A and D in S1a.

357

Facies associations	S1a	S1b	S1c	Facies code	Sedimentary characteristics	Depositional environment
E		F1U1		Br	Coarse (cobble and boulder) limestone breccia	Cryogenic brecciated cave fill
D	F1U2	F1U2	F1U2 F1U3	Gm, Sfl	Massive beds of gravel (pebble)	Gravel deposition by unconstrained

	F3U1 (base)		F2U3		tabular in form with occasional weakly developed horizontal stratification (Gm), occasional sand beds (massive or cross-bedded) with drapes of silt/clay (flaser type; Sfl)	current flow with periods of sand deposition associated with current flow processes
C	F3U2 F4U1			Gch	Massive and homogeneous gravels (pebble) set within steep-sided channel/gully forms	Gravel deposition within entrenched gullies. The phases of entrenchment are associated with a lowering of base level and erosional re-adjustment, or a very high energy flood event
B	F5U3 F6U1 F6U3		F1U1 F2U2	Gs	Stratified beds of gravel (pebble) exhibiting steep (>30°) stratification	Gravel deposition in association with distal deposits of steep-angled talus cones
A	F1U1 F1U3 F2U1-3 F3U1 F3U3 F4U2 F4U3 F5U1 F5U2 F6U2 F6U4	F1U3	F2U1	Sfl, Flt	Beds of sand (massive or cross-bedded) with drapes of silt/clay (flaser type; Sfl) and beds of silt/clay (Flt) with occasional sand laminations (ca. 1 mm thick) and occasional sand lenses (up to 5 cm thick)	Sand deposition in association with current flow processes in a subaqueous environment characterised by episodic still-water conditions with fine-grained sedimentation dominated by rainout of material from suspension

358 Table 1. Description and interpretation of the sedimentary facies observed in the
359 sections through the Siliceous Member in Westbury Cave.

360

361 3.2. Particle size analysis

362 The samples taken for particle size analysis are poorly, very poorly or extremely
363 poorly sorted, as determined by analysis in GRADISTAT (see Supplementary

364 Material for particle size analysis raw data and GRADISTAT outputs). The gravels of
365 facies associations C and D contain similar proportions of gravel-sized material (55-
366 60%) and are all very fine (2-4 mm) gravels, except the medium (8-16 mm) gravel of
367 sample F1U2a from facies association D (see Supplementary Material Fig. S3). The
368 mean size of sample F3U2a (facies association C) is, however, ca. 500 μm less than
369 the other very fine gravels. The coarse unit of facies association B (F5U3) has
370 comparably lower gravel content (20%) compared with the other coarse units in S1a,
371 and is strictly a 'gravelly muddy coarse sand', rather than a coarse unit dominated by
372 gravel-sized sediments. The majority of the fine-grained sediments of facies
373 association A are classified as 'clayey silts'.

374

375 **3.3. Clast lithology**

376 The >16 mm clast fraction of the facies association B coarse unit (F5U3; Table 2) is
377 dominated by chert (75%), a spicular chert (21%) lithologically similar to Cretaceous
378 Upper Greensand Fm chert, and limestone (4%). The 8-16 mm fraction is also
379 dominated by chert (48%) and spicular chert (21%), and also contains limestone
380 clasts (5%). Additional lithologies present in the 8-16 mm fraction include
381 Carboniferous fossils such as corals (11%), Carboniferous chert (5%), vein quartz
382 (8%), and quartzite (1%).

383

384 Cherts also dominated the coarse-grained units in F4 and F1 (facies associations C
385 and D), but in different proportions (Table 2). Carboniferous and undifferentiated
386 cherts make up the majority of clasts in the F4U1 gravels (facies association C): 50%
387 each in the 16-32 mm fraction, 28% and 65% in the 8-16 mm fraction, respectively.

388 The only other lithologies present in small numbers in the F4U1 gravels include

389 spicular chert (3%), Carboniferous limestone fossils (1%), and phosphate (3%). The
 390 F1U2 gravel (facies association D) has a larger proportion of spicular chert (54% in
 391 16-32 mm fraction, 11% in 8-16 mm fraction), with considerable numbers of clasts of
 392 undifferentiated chert (38% in 16-32 mm, 42% in 8-16 mm) and Carboniferous chert
 393 (8% in 16-32 mm, 34% in 8-16 mm). Similar to F5U3, the F1U2 gravel also contains
 394 vein quartz (11%) and quartzite (1%). No Carboniferous limestone clasts were found
 395 in either F4 or F1 gravels, with a very small proportion of clasts being limestone
 396 fossils (1%).
 397

Lithology categories		Lithology	F5U3 (facies association B)		F4U1 (facies association C)		F1U2 (facies association D)	
			16-32 mm (%)	8-16 mm (%)	16-32 mm (%)	8-16 mm (%)	16-32 mm (%)	8-16 mm (%)
Local	Durable	Chert	75	48	50	65	38	42
		Carboniferous chert	-	5	50	28	8	34
		Vein quartz	-	8	-	-	-	11
	Non-durable	Carboniferous limestone	4	5	-	-	-	-
		Carboniferous limestone fossils	-	11	-	1	-	1
Non-local	Durable	Spicular chert (Upper Greensand?)	21	21	-	3	54	11
		Quartzite	-	1	-	-	-	1
		Phosphate	-	-	-	3	-	-
		Unknown	-	1	-	-	-	-
		<i>n</i>	<i>24</i>	<i>300</i>	<i>2</i>	<i>192</i>	<i>26</i>	<i>412</i>

398 Table 2. Clast lithology results of samples taken from three coarse-grained units
 399 (F5U3, F4U1, F1U2) through Section 1a of the Siliceous Member in Westbury Cave.
 400

401 3.4. Palaeomagnetic dating

402 The Siliceous Member sediments exhibit magnetic susceptibility values ranging from
403 $50-90 \times 10^{-6}$ SI units/vol. with a median value of 65×10^{-6} SI units/vol. indicating
404 sufficient magnetite content for palaeomagnetic analysis. Palaeomagnetic
405 remanence measurements made after alternating field demagnetisation, typically in
406 the range of 10-100 mT, indicate that most of the samples ($37/52 = 71\%$) reveal a
407 single (primary) stable reversed component of remanent magnetisation. Median
408 destructive fields (MDF) are in the range of 20-80 mT (Fig. 9), typical of magnetite-
409 bearing sediments. While most samples appear to contain predominantly single-
410 domain magnetite, about one-third exhibit soft magnetisation indicative of multi-
411 domain magnetite (MDF < 20 mT), and most samples also appear to contain small
412 amounts of hematite. Fifteen samples, not from any particular face, have low NRM
413 values (< 0.3 mA/m), and reveal poor quality records, probably due to coarser
414 textures (multi-domain magnetite grains), but are nevertheless reversely magnetised.
415 The mean inclination (all samples; Fig. 10) is about 15 degrees shallower than
416 expected for the Geocentric Axial Dipole (GAD) field at this latitude (-68° for a
417 reversed field at 51.25° N latitude). This is likely due to inclination flattening of
418 magnetic grains, a feature which is often encountered in older lacustrine sediments,
419 and thought to be due to compaction (Verosub, 1977; Verosub et al., 1979; Butler,
420 1992). All sampled sediments of the Siliceous Member are reversely magnetised
421 (Fig. 10; Table 3) and based on stratigraphical and other geochronological evidence,
422 can be confidently assigned to the Matuyama Reversed Chron (2.58-0.78 Ma).

423

Face number	n	<i>D</i>	<i>I</i>	<i>k</i>	α_{95}	P	Chron
F1	8	204	-58	19	13	R	Matuyama
F2	10	198	-60	21	11	R	Matuyama
F3	8	232	-52	12	17	R	Matuyama
F4	7	196	-46	31	11	R	Matuyama

F5	4	192	-35	263	6	R	Matuyama
Means							
all units	5	204	-51	30	14	R	Matuyama
all samples	37	205	-53	15	6	R	Matuyama
GAD		0	-68				
PEF		358	66				

424 Table 3. Summary of palaeomagnetic direction. *n*, total number of specimens used
425 from each face; *D* and *I*, declination and inclination of the mean direction in degrees;
426 *k*, precision parameter; α_{95} (degrees), circle of confidence ($p = 0.05$); P, polarity (R =
427 reversed). The mean inclination expected for geocentric axial dipole (GAD) at this
428 sampling latitude (51.25°N) is -68° for a reversed field. Present Earth's field (PEF)
429 direction at sampling locality: *D* = 2° westerly, *I* = 66°N.

430

431 4. Interpretation

432 4.1. Depositional model

433 The stratigraphy of the Siliceous Member presented here has revealed previously
434 unrecognised complexity. Originally described as a single, 10 metre-thick unit of
435 sands and gravels, it is now apparent that the Siliceous Member also contains
436 substantial thicknesses of finer-grained clay and silt. Although previous investigators
437 did note clay/silt in the upper 1.5 metres of Siliceous Member sediments (Andrews
438 and Cook, 1999), considering them 'cap muds' attributed to the final waning stages
439 of fluvial activity, the presence of fine-grained material over seven metres from the
440 top of the Siliceous Member has not previously been recorded. A discussion of the
441 sequence is presented below to inform a new depositional model.

442

443 The presence of cross-bedded sands in facies associations A and D, gravel lenses
444 with channel architecture in facies association C, and many well-rounded gravel
445 clasts in facies associations B, C and D in Siliceous Member sediments are features

446 of subaqueous deposition, and agree with previous interpretations suggesting that
447 the sediments are water-lain (Stanton, 1973, 1999; Bishop, 1982). The rare
448 limestone boulders (visible in Figs. 5k and 7e) reflect large blocks spalling from the
449 cave walls and roof.

450

451 Stanton (1999) believed that sinkholes, formed by the dissolution of limestone
452 bedrock, formed the surface entrances into Westbury Cave with progressive cave
453 enlargement under phreatic conditions. Indeed, stream sinks have been shown to
454 feed many cave systems with large quantities of sediment (Farrant & Smart, 2011).
455 Although the temporal relationship between cave formation and Siliceous Member
456 deposition is unknown, Bishop (1982) suggested that a significant period of time
457 elapsed after phreatic cave formation and before deposition of the Siliceous Member
458 (see below). Under vadose conditions (above the water table), water would have
459 accumulated at the cave base if full drainage were impeded for any reason. Standing
460 water would have led to lake-style deposition at this point in the cave's development.
461 The characteristic distal deposits of lakes include rainout of clay/silt-sized particles
462 from suspension under quiescent conditions, and coarser sand and gravel units
463 derived from fluvial stream inputs (Talbot & Allen, 1999). Entrance talus is also
464 another important source of coarse-grained deposition in caves (White, 2007), and
465 palaeontological remains are often found within these poorly stratified talus gravels
466 (White, 2012). Winnowing of finer-grained material and buoyant fossils from proximal
467 poorly-sorted sediments can result in finer-grained, better sorted, fossil-rich gravels
468 and sands being washed deeper into cave systems as distal deposits (e.g., Pickering
469 et al., 2007). If deposition occurred under phreatic conditions (below the water table)
470 and the cave was entirely water-filled, the clay/silt-sized particles would settle out

471 from suspension in the same way during periods of quiescence, with coarse material
472 being fed into the cave when flow energy was higher, with preference for gravel
473 deposition in areas where cave passage cross-sectional area was small. Places
474 where passage cross-sectional area are small are known to be areas of higher flow
475 velocity since, for a given discharge, velocity varies inversely with passage cross-
476 sectional area (Van Gundy and White, 2009). In these areas of higher velocity,
477 coarser material could be transported but as passage cross-sectional area increases
478 again after constrictions and as velocity correspondingly decreases, coarse material
479 could no longer be transported and would be deposited.

480

481 Whether the Siliceous Member was deposited under phreatic or vadose conditions
482 has been a subject of debate. Stanton (1973, pg. 289) noted that “rock walls in the
483 lower part of the pit show original phreatic features” and suggested (pg. 291) that the
484 Siliceous Member “accumulated under water until the lower half of the chamber was
485 full”. However, Bishop (1982, pg. 13) noticed “the presence of a small series of rills
486 incised into the upper surfaces of limestone bedrock associated with Bed 1
487 [Siliceous Member]” and he interpreted these features to mean that “sand-laden
488 water was entering the system from the west side, and was running over the
489 exposed bedrock above any standing water” and he linked this to deposition under
490 vadose conditions. He argued that the phreatic features, such as wall scalloping,
491 were superimposed by vadose features associated with Siliceous Member
492 deposition, and that phreatic features were created during initial phreatic cave
493 development that pre-dated the Siliceous Member by some unknown amount of
494 time. Although Stanton (1999) acknowledged this conflict, he did not resolve it nor
495 provide additional evidence supporting either case, only summarising his view (pg.

496 18) that “Under phreatic low-gradient conditions the streamborne sediments would
497 not have penetrated far into the cave at first, so large empty solution cavities would
498 have formed. As the stream cut down and opened new entrances into these cavities,
499 gravel, sand and silt would have been washed into them, forming the Siliceous
500 Member.”

501

502 The evidence presented here cannot resolve this debate. The walls of the cave were
503 not accessible during our excavations and were less well exposed than during
504 Stanton’s and Bishop’s earlier studies and so could not be further investigated.
505 Boulders encountered during excavation were a mixture of angular and more
506 rounded blocks of limestone, but none were obviously scalloped. The rounding of
507 some boulders indicates erosion by solution. This process may be more common in
508 phreatic systems, but could also occur when water flows over and around boulders
509 under vadose conditions.

510

511 The model for Siliceous Member deposition proposed here is similar to that outlined
512 by Martini (2011) for Mugnano Cave in Italy, which was suggested to have filled by
513 quiet deposition in a subterranean lake with occasional sediment-laden floods. The
514 sediments described from the Siliceous Member also have many of the features
515 mentioned by Gillieson (1986) as indicative for standing water (e.g., horizontal or
516 inclined stratification, and cross-stratification with flame structures—as in facies
517 association A) and cave stream deposition (e.g., cross-stratified gravels and
518 horizontal discontinuous stratification—as in facies associations C and D) at various
519 depositional energies. The Siliceous Member sediments also conform with several
520 facies types listed by Ford (2001) as typical cave sediment types (see his figure 2,

521 pg. 9), including: Lp – “laminated clays and silts due to ponding effects of surface
522 lakes” and Lb – “silts and muds in abandoned phreatic systems” (facies association
523 A); Wg – “winnowed gravel below inlets” (facies association B); and Ag – “gravel in
524 contemporary stream” and As – “sand in contemporary stream” (facies associations
525 C and D).

526

527 Evidence from Siliceous Member sedimentology points to changes in process
528 upwards through the section. Facies association A is found in all sections from the
529 base of S2 to the top of S1a, and represents the standing water deposits (denoted
530 by clayey silt) of a subterranean lake if vadose conditions prevailed, or a submerged
531 cave conduit under phreatic conditions. This standing water was episodically fed by
532 flow from streams on the land surface that discharged into the karstic environment
533 (sands, and occasional gravels, such as in S2 and in S1a F6U3). The thick sands
534 and gravels of facies association B dip relatively steeply (ca. 30 degrees) and it is
535 likely that these represent winnowed, distal deposits of coarser, proximal deposits
536 associated with entrance talus slopes that were fed from a cave entrance higher up.
537 This model has been applied to other cave systems, such as the hominin-bearing
538 caves of South Africa, where entrance talus has been hydrodynamically transported
539 deeper into the cave along with palaeontological remains (Pickering and Kramers,
540 2010). The thin sand lenses within facies association B in S1a F5U3 and S1c F2U2
541 suggest that small streams occasionally flowed over this talus slope between the
542 higher energy events that deposited the thick gravelly coarse sands. A similar
543 winnowing of coarser deposits near the cave entrance is possible under phreatic
544 conditions and the gravels may have resulted from increased flow around boulders
545 on the passage floor (see rounded boulders adjacent to the facies association B

546 gravels in Figs. 5e, 5k, 7b, 7e). Thinner sand lenses may result from localised
547 increases in flow rate or from short-lived increases in flow velocity through the
548 conduit.

549

550 The erosional contact at the base of S1a F5U1/ S1c F2U1 clay (498 cm below
551 datum, B.D.) is likely to have been produced by a high-energy flood event that
552 scoured into the underlying gravels. The coarse deposits of this high-energy event
553 cannot be identified in the faces studied here, but were probably transported deeper
554 into the cave downslope. The extensive clayey silts of facies association A in S1a
555 units F5U1/F4U3/F3U3 (257-498 cm B.D.) represent a long period of stable, fine-
556 grained deposition in a subterranean lake or submerged cave conduit setting, with
557 sand lenses representing repeated inputs of coarser sediments from in-wash events.
558 The truncating angular unconformity at the base of S1a F3U2/F4U2 was produced
559 by another, much larger erosional event, such as a very large flood event with
560 enhanced scour. Catastrophic lake drainage has also been invoked in previous
561 studies for similar unconformities in clastic cave sediments by Martini (2011), who
562 suggested that a similarly high-relief erosional surface between clastic cave
563 sedimentary units was related to a fall in lake level. If phreatic conditions prevailed,
564 then drainage of the submerged conduit could have facilitated a switch from
565 depositional to powerfully erosional regimes. As with the erosional contact at 498 cm
566 B.D., the products of this event must have been transported deeper into the cave, as
567 the coarse sediments responsible for the extensive scour are not seen directly above
568 the contact, except perhaps for the gravel lens near the base of the unconformity in
569 S1a F4. These shifts between erosional and depositional regimes are characteristic

570 of allochthonous cave sedimentation, and resultant “cut and fill” structures are
571 common phenomena (Simms, 1994).

572

573 Another phase of fine-grained deposition, with similar sand in-wash events, then
574 began on this inclined erosional surface, creating the angular unconformity. This
575 suggests cave lake, or fully submerged conduit, conditions were re-established as
576 before. The particle size of the facies association C gravels is larger than the facies
577 association B gravelly sand units and the beds are less steeply dipping. These
578 characters are more comparable to the cave stream thalweg or channel facies
579 described by Bosch and White (2004). This facies change could indicate a change in
580 the location of sediment input into the cave, in the configuration of the cave passage,
581 or in the nature of the cave flow regime. Rather than being coarse gravels, the facies
582 association C gravels are very fine-medium gravels and as such may represent
583 distal channel flood deposits, or under phreatic conditions a flooding event of only
584 moderate energy.

585

586 S1a F3U1 (278 cm B.D.) marks a return to lower-energy standing water deposition
587 (i.e., the slack-water facies sensu Bosch and White, 2004) with sporadic high-energy
588 in-wash of gravels/sands continuing up into S1a F2U3. The increase in sand content
589 and extent of sand beds up S1a F2 suggests that lake-style deposition was gradually
590 overtaken by fluvial-style channel deposition. This could be explained by a shift in
591 flow regime from low energy standing water deposition to consistent flow passing
592 through the cave chamber, whether as cave streams under vadose conditions or as
593 coarse inputs through a submerged conduit under phreatic conditions. The facies
594 association D gravels and cross-bedded sands above in S1a/S1b F1U2 indicate a

595 sustained period of high-energy flood events with high erosive power, exemplified by
596 the presence of over eight unconformities. These gravels have a similar
597 sedimentological character (colour, dip, particle size) to the facies association C
598 gravels but occur in large tabular beds indicating deposition from an unconstrained
599 flow unlike the facies association C gravels. Gravels of both facies associations C
600 and D often have flame structures (e.g., S1a F3U2/F4U1 gravels; Fig. 5c-d) and load
601 casts (e.g., S1c F2U2 gravels; Fig. 7b) at their lower contacts, indicating subaqueous
602 soft sediment deformation from rapid deposition of the denser gravels onto the
603 underlying silts and sands. It is likely that S1a F1U1 and F1U3 are not in situ, as they
604 have several characteristics of slump deposits (Huggett, 2011), such as irregular
605 margins representing slip planes and internal folds and faulting resulting from
606 rotational movements.

607

608 The eastern extension of S1a F1 to produce S1b exposed the contact between the
609 facies association D sediments that comprise S1a/S1b F1U2 and the overlying
610 sediments of S1b F1U1—a coarse (cobble/boulder) limestone breccia with a
611 red/brown clay matrix (facies association E). The sedimentary properties of the
612 breccia are typical of those of the early Middle Pleistocene cave breccias of the
613 Calcareous Member (Andrews and Cook, 1999). The contact is irregular, steeply
614 dipping and cuts into the underlying Siliceous Member deposits of S1b F1U2. This
615 contact represents the boundary between the Siliceous and Calcareous Members
616 and the uppermost contact of the Siliceous Member. Due to poor exposure, it is not
617 possible to elaborate here on discussions of the Siliceous-Calcareous Member
618 boundary by Stanton (1973, 1999) and Bishop (1982), who suggest it appears to
619 represent a period of non-deposition, roof collapse, and cave drainage. However, the

620 complexities of this important boundary have not previously been documented in
621 detail.

622

623 The sequence exposed in S2 records similar sedimentary characteristics to the
624 deposits of S1. The cleared section of S2, being approximately 50 cm wide, did not
625 allow for a detailed investigation into the lateral complexity of these deposits as was
626 the case in S1. The occurrence, in this section, of interbedded units of clay, silt,
627 sands and gravels of facies associations A and D can be used to infer that the
628 existence of a still, lacustrine environment or submerged cave conduit fed by
629 episodic pulses of stream flow that delivered coarser-grained sediments into the
630 karstic setting. Therefore, the implied model for the accumulation of the sediments in
631 S1 was also responsible for the accumulation of the sediments of S2.

632

633 **4.2. Sediment provenance**

634 The gravel-rich facies contain a range of lithological types that can be broadly
635 divided on the basis of the modern distribution of geological strata in southern and
636 western England, into durable and non-durable as well as local and non-local rock
637 types. Durable clast types are those that can sustain routine and persistent bedload
638 transportation. As shown in Table 2, facies association B gravels are the only gravels
639 to contain non-durable lithologies (Carboniferous limestone and limestone fossils) to
640 any extent: 4% in the 16-32 mm fraction and 16% in the 8-16 mm fraction, compared
641 to 0% in the 16-32 mm fraction and 1% in the 8-16 mm fraction for the facies
642 associations C and D gravels. The facies associations C and D gravels contain more
643 durable lithologies (chert, Carboniferous chert, vein quartz, spicular chert – see
644 Table 2). It is likely that the presence/absence of non-durable lithologies is a function

645 of sediment process creating a taphonomic bias. In deposits laid down by genuine
646 stream flow processes (facies associations C and D), the high energy
647 abrasion/attrition of the bedload will rapidly remove non-durable clasts from the
648 sediment, resulting in an exclusively durable clast population. In contrast, in deposits
649 laid down by a combination of stream flow and more local talus cone development
650 (facies association B), the restricted transport distance will also allow the
651 preservation of non-durable clast types.

652

653 Local rock types reflect the range of lithologies that can be derived from the
654 underlying bedrock and immediate local area (within only a few km) based on
655 modern outcrop patterns. These include limestone, coral fossils, and chert from
656 Carboniferous rocks immediately surrounding the cave, and possibly vein quartz,
657 which may also derive from the Carboniferous limestone or from nearby Devonian
658 sandstone outcrops at North Hill, east of Priddy (Fig. 3). The non-local rock type is
659 primarily a spicular chert, very similar to cherts derived from the Cretaceous Upper
660 Greensand Formation, which is highly durable. Most gravel units (particularly facies
661 associations B and D) contain a mixture of both local and non-local lithologies, while
662 facies association C gravels seem to contain more local lithologies (100% and 94%
663 are local in the 16-32 and 8-16 mm fractions, respectively).

664

665 Cherts are the dominant lithology in the sequence and can be divided into three
666 distinct lithological types: 1) Carboniferous chert, 2) spicular chert and 3)
667 undifferentiated chert. Much of the undifferentiated chert, which is of a dark grey
668 colour, could simply be Carboniferous chert that lacks distinguishing fossils but could
669 also be derived from the Jurassic Harptree Beds that outcrop in several locations

670 across central Mendip (Green and Welch, 1965; Bishop, 1982). Although not found
671 at the site of Westbury itself, these would still be of relatively local derivation.

672 Carboniferous chert is distinguished on the basis of the “letter-box” shaped crinoid
673 impressions that are distinctive of cherts of this age. These cherts are local in origin
674 and are likely derived from the underlying bedrock. As mentioned above, the spicular
675 cherts are similar to those derived from the Upper Greensand Formation that
676 outcrops across southern England (Stanton, 1973, 1999; Bishop 1982). Cretaceous
677 strata are absent from much of the area and have only recently been discovered in
678 situ on the eastern Mendip Hills, 17 km from Westbury Quarry at Tadhil (Farrant et
679 al., 2014), with the nearest other outcrops of the Upper Greensand Formation lying
680 some 24 km to the southeast of Westbury Cave at Postlebury Hill and around 30 km
681 to the Upper Greensand Formation escarpment around Frome (Fig. 3). The
682 phosphate clasts may also derive from Cretaceous strata, since phosphatic nodules
683 are common in certain parts of the Upper Greensand Formation and basal Chalk
684 Group succession, particularly the Glauconitic Marl Member of the West Melbury
685 Marly Chalk Formation in the Grey Chalk Subgroup (Hopson et al., 2001), which also
686 crops out near Frome (Fig. 3). It has been argued that Cretaceous strata previously
687 covered the Mendip Hills in their entirety and that these strata have been removed
688 by progressive denudation, although the timing of this denudation is not precisely
689 known (Donovan, 1969; Farrant et al., 2014). Consequently, it is unclear whether the
690 Upper Greensand-like chert that accumulated in Westbury Cave at the time of
691 accumulation of the Siliceous Member was of local (within a few km of the cave) or
692 far-travelled origin (from other parts of the Mendip Hills or even outside the region).

693 However, Stanton (1973; 1999) has suggested that the roundedness of Upper
694 Greensand chert clasts could result from them being reworked from now denuded

695 outcrops of Cenozoic conglomerates in the vicinity of Westbury Cave. Nevertheless,
696 he also noted that the quartz in sand layers of the Siliceous Member appeared more
697 similar to quartz from the Upper Greensand Formation than the Old Red Sandstone
698 or the Millstone Grit (Stanton, 1973), suggesting probable provenance from
699 Cretaceous outcrops. The high content of spicular chert could, on the basis of
700 modern outcrop distribution, imply that the Siliceous Member represents deposits of
701 a subterranean fluvial network with a relatively extensive catchment fed from
702 channels flowing from the south or east of the region, where the nearest outcrops of
703 the Upper Greensand Formation currently occur. However, the progressive erosion
704 of Cretaceous strata could also mean that the lithological assemblage of these
705 deposits can be explained by the activity of an entirely local system of restricted
706 catchment draining remnant outcrops of the Upper Greensand Formation, and
707 possibly Cenozoic conglomerates, on the Mendip plateau in the vicinity of the cave.
708 Given the supposed widespread coverage of the Mendip Hills by Cretaceous strata,
709 the latter is probably the most likely but the former cannot be discounted.

710

711 The absence of certain clast lithologies is also of interest. For instance, the lack of
712 Devonian sandstone clasts from the Portis Head Formation suggests that the
713 Devonian inliers of the Mendip Hills were not exposed at the time of Siliceous
714 Member deposition and did not form part of the Siliceous Member catchment. In
715 addition, the rarity of autogenic limestone clasts in facies association B gravels and
716 their complete absence in facies association C and D gravels suggests either these
717 clasts were originally present but were broken up or dissolved completely during
718 transport and/or in situ, or that few autogenic limestone clasts were generated in the
719 first place. The second scenario might support the view of deposition in a phreatic

720 cave conduit rather than a vadose cave stream, where active collapse and autogenic
721 limestone clast production would be more common, and would suggest that the
722 hydraulic gradient of the cave system was low. If the hydraulic gradient (the change
723 in hydraulic head, i.e. the energy possessed by a unit weight of water, between two
724 points) is high, then steep passage profiles will form as the flow cuts down to an area
725 of lower hydraulic head, exposing and eroding the rocks making up the cave walls
726 and generating autogenic clasts. If the hydraulic gradient is low, as is often the case
727 in phreatic passages, the rocks of the cave walls are not exposed or eroded as
728 readily and passage profiles are not as steep (Palmer, 1991).

729

730 **5. Discussion**

731 The palaeomagnetic analysis carried out in this study has yielded robust evidence
732 for reversely magnetised sediment at every level that was analysed (Figs. 8-10).
733 These data place the Siliceous Member of Westbury Cave securely before the
734 Brunhes-Matuyama boundary (0.78 Ma) and within the Early Pleistocene. The new
735 analysis supports older, unpublished palaeomagnetic studies, also consistent with
736 the Siliceous Member being deposited during the Early Pleistocene (Yassi, 1983,
737 Farrant, 1995) and existing biostratigraphical data that indicate that these sediments
738 were laid down in the Early Pleistocene (Bishop, 1982; Gentry, 1999). Given the
739 paucity of fossil-bearing sediments in the British Isles that relate to this time interval,
740 Westbury Cave thus represents a unique site that requires further investigation.

741

742 The Siliceous Member provides one of the few fossil records for the Early
743 Pleistocene outside East Anglia in Britain and possibly from an interval not
744 represented by other British sites (Fig. 1). However, the precise provenance of fossil

745 material recovered from the Siliceous Member by past workers (Bishop, 1982) is
746 unclear and cannot be related to stratigraphy within the Siliceous Member. The new
747 depositional model considered here importantly suggests differences in both source
748 material transport distance and taphonomy between coarse-grained units.

749

750 Previous studies have suggested that the sediments of the Siliceous Member at
751 Westbury-sub-Mendip reflect deposition mainly by a subterranean river. However,
752 this study shows that the Siliceous Member is dominated by fine-grained silts/clays
753 (facies association A) deposited in a vadose still-water lacustrine or phreatic fully
754 submerged conduit environment that was fed by episodic influxes of stream flow
755 (either from a subterranean river system or by input from a surface system that was
756 discharging into the karstic environment) and talus cones (fed by surface sediment
757 derived from cave entrances). If the Siliceous Member was deposited under phreatic
758 conditions it is possible that the sequence developed by upward aggrading
759 paragenesis (sensu Farrant and Smart, 2011), when sediment builds up on the cave
760 floor of a submerged conduit and erodes upwards into the soluble limestone to
761 create accommodation space for further sedimentation. In this situation, variable flow
762 rates result from changing sediment input, stream discharge, and dissolution. Under
763 phreatic conditions, it is also possible to have coarse inputs with more far travelled
764 lithologies (e.g., facies associations C and D) as well as coarse inputs with a more
765 local component (e.g., facies association B). The main elements of the proposed
766 depositional model are: 1) facies association A: massive/laminated silts/clays that
767 reflect rainout of material from suspension in a still water environment, 2) facies
768 association B: steeply dipping gravels beds (containing local and non-local, durable
769 and non-durable clast types) that likely represent distal talus deposits derived from

770 cave entrance material (either the cave mouth or the entrance of pipes/tubes with a
771 connection to the land surface into the cavern), 3) facies association C:
772 sands/gravels infilling incised channel forms that represent sediment infilling of gully
773 features that develop after phases of incision probably associated with episodic
774 drainage/desiccation of the lake or conduit system, and 4) facies association D:
775 sands/gravel lenses/beds (dominated by local and non-local, durable clast types)
776 that represent higher energy inflow from surface or sub-surface systems.

777

778 The alternation between these different facies is most likely to have been caused by
779 autocyclic variations within the lake/fluvial system under vadose conditions, or due to
780 variation in flow caused by changing conduit cross sectional area and discharge
781 under phreatic conditions, rather than through allocyclic climatic control. This means
782 that the accumulation of sediments can be explained by internal functions of the
783 sedimentary system, i.e. the cave system itself, without the need to invoke external
784 controls, such as changes in climate. The exception to this is the downcutting
785 associated with the gully features. These clearly record major changes in the lake or
786 submerged conduit environment but whether these reflect a complex response of the
787 subterranean hydrological system or some wider environmental driver is unclear.
788 Palaeoenvironmental proxy evidence from each of the different facies combined with
789 a well-constrained chronology for the sequence would be required to offer insight
790 into whether extrinsic, climatic or environmental controls were influencing deposition.
791 For example, Lewis et al. (2001) used sedimentological facies changes in
792 combination with pollen analysis and radiocarbon and OSL dating to demonstrate
793 that fluvial systems were responding to Late Pleistocene rapid climatic changes.

794

795 In the context of cave sedimentation, climatic drivers on sedimentation have been
796 considered to control shifts between speleothem formation and clastic sedimentation
797 in caves from other parts of the world, mostly based on comparing well-dated
798 episodes of speleothem growth with regional or global records of climatic and
799 environmental change (e.g., Moriarty et al., 2000; Pickering et al., 2007, 2011).
800 Stable isotopes have also been used on cave sediments to suggest shifts in
801 vegetation types concurrent with changes in cave facies (Pickering et al., 2007).
802 Westbury Cave lacks speleothems associated with the Siliceous Member, so these
803 cannot be used for stable isotope or dating analyses, and spot samples taken from
804 the silts/clays of facies association A for pollen analysis were barren. Fossil mammal
805 assemblages are the only palaeoenvironmental proxy record recovered from the site
806 thus far but are apparently restricted to the coarse-grained deposits. Palaeomagnetic
807 dating provides a broad chronological constraint so attempting other absolute dating
808 methods at the site (such as cosmogenic nuclide or U-series/ESR dating) will likely
809 prove important in future.

810

811 This new understanding of the depositional environment of the Siliceous Member
812 has implications for the fossil assemblages derived from these sediments. The
813 gravel-dominated units (such as those seen in facies associations B, C, D) are the
814 most likely sediments to contain fossils, as significant current flow is required to
815 entrain and transport bone/fossil material into the cave environment, and indeed all
816 previously reported fossils have come from coarse-grained units of the Siliceous
817 Member. However, the gravel-dominated beds themselves reflect sedimentation by a
818 range of processes with concomitant implications for the taphonomy of the contained
819 assemblages. Previous work on the Siliceous Member fossils indicate that they are

820 frequently rolled and heavily abraded (Bishop, 1982; Andrews and Ghaleb, 1999).
821 Given the sedimentology of the gravel deposits described here, this is unsurprising,
822 as many of these were deposited by high-energy currents moving gravel-sized clasts
823 as bedload, resulting in rounding and breakage of fossil remains. It is also likely that
824 such processes would favour the preservation of teeth and tooth fragments over
825 bone as the hard-wearing enamel that constitutes dental material would be more
826 resistant to high-energy current transport (Behrensmeyer, 1988). This is also
827 consistent with current understanding of the Siliceous Member fossil assemblage,
828 which is dominated by teeth and tooth fragments (Bishop, 1982; Andrews and
829 Ghaleb, 1999). Although the sand and gravel beds (e.g., facies association C and D)
830 may yield rolled/abraded fossils, the distal talus deposits (facies association B) might
831 be expected to contain better preserved fossils as the transport distance over which
832 these sediments are moved will be significantly shorter, thus reducing the potential
833 for bones and teeth to sustain damage. This could also be true under phreatic
834 conditions if cave inputs were more locally derived during a certain period of
835 deposition. A complex assemblage containing both well-preserved and poorly-
836 preserved fossils would therefore be anticipated. From the limited work carried out
837 on the Siliceous Member assemblages to date by previous workers, varying degrees
838 of rolling, abrasion and preservation seem to be a key attribute of fossils from these
839 sediments (Bishop, 1982; Andrews and Ghaleb, 1999), thereby upholding this
840 interpretation.

841

842 It is also important to note that the episodic drainage of the lake environment or
843 flooding of the submerged conduit and the associated incision into the underlying
844 sediments may have resulted in the reworking of older fossils from within the

845 Siliceous Member, as evidenced by the often erosive contacts between facies
846 associations C, D and A. The span of time represented by the Siliceous Member is
847 not known. However, if any significant time depth is represented, it would not be
848 unrealistic, given the evidence for episodic downcutting within this unit, for single
849 beds to contain conflated assemblages of a mixture of ages and/or
850 palaeoenvironmental conditions.

851

852 **6. Conclusions**

853 The Siliceous Member in Westbury Cave is dominated by fine-grained silts/clays with
854 interbedded lenses/beds of sands and gravels. The characteristics of the Siliceous
855 Member are, therefore, more consistent with sediment deposition within a
856 subterranean lake under vadose conditions or a submerged conduit under
857 paragenetic, phreatic conditions fed by current flow dominated surface or sub-
858 surface systems than with a single subterranean fluvial system, as was previously
859 suggested. The sediments contain a wide-range of clast lithologies, several of which
860 are not currently local to the immediate area. However, it is unclear whether this is
861 because the cave system was fed by a river system with a spatially-extensive
862 catchment that included non-local lithologies, or because these now non-local
863 lithologies outcropped in the vicinity of the cave during the Early Pleistocene but
864 have since been removed by denudation in the region (the most likely option given
865 recent evidence of Cretaceous overstep of the Mendip Hills). The palaeomagnetic
866 polarity data, when combined with the existing faunal evidence, strongly suggests
867 that the Siliceous Member is of Early Pleistocene age, one of the few sites that can
868 be correlated with this interval outside of the Crag Basin of East Anglia.
869 Consequently, the Siliceous Member is unique in its potential to increase our

870 understanding of the Early Pleistocene in Britain. Further work on this site will
871 increase our understanding of both its age/stratigraphical position and the
872 palaeoenvironments that existed during its accumulation.

873

874 **Acknowledgments**

875 N.F.A. thanks the Royal Holloway Academic Awards Group for the award of an Irene
876 Marshall Scholarship, which funded fieldwork in Westbury Quarry in June-July 2014,
877 and the Palaeontological Association for funding fieldwork in April 2016 through the
878 Callomon Award (grant PA-CA201501). The authors thank Natural England for
879 funding as part of the Geological Conservation Review, which supported fieldwork in
880 December 2015. The authors would also like to thank: Alford Technologies Ltd. and
881 Natural England, for access to land and permission to conduct this research; Nigel
882 Taylor, for extensive logistical support during fieldwork in Westbury Quarry; Pierre
883 Schreve, Luke Parker and Tom White, for assistance in the field; and Adrian Palmer,
884 for help with particle size analysis. We thank the three anonymous reviewers for their
885 detailed comments and suggestions that improved the manuscript.

886

887 **References**

888 Andrews, P., Cook, J., 1999. Description of the sedimentary sequence in Westbury
889 Cave. In: Andrews, P., Cook, J., Currant, A., Stringer, C. (Eds.), Westbury Cave: The
890 Natural History Museum excavations 1976-1984. Western Academic & Specialist
891 Press Ltd., Bristol, pp. 19-58.

892

893 Andrews, P., Cook, J., Carrant, A., Stringer, C., 1999. Westbury Cave: The Natural
894 History Museum excavations 1976-1984. Western Academic & Specialist Press Ltd.,
895 Bristol, pp. 309.
896
897 Anon., 1917. Miscellaneous. Geological Magazine 4, 480.
898 doi:10.1017/S0016756800136519.
899
900 Antoine, P., 1990. Chronostratigraphie et environnement du Paléolithique du Bassin
901 de la Somme. Publications du Centre d'Études et de Recherches Préhistoriques 2,
902 1-231.
903
904 Ashton, N., Lewis, S.G., De Groote, I., Duffy, S.M., Bates, M., Bates, R., Hoare, P.,
905 Lewis, M., Parfitt, S.A., Peglar, S., Williams, C., Stringer, C., 2014. Hominin
906 footprints from Early Pleistocene deposits at Happisburgh, UK. PLoS ONE 9,
907 e88329. doi:10.1371/journal.pone.0088329.
908
909 Arzarello, M., Pavia, G., Peretto, C., Petronio, C., Sardella, R., 2012. Evidence of an
910 Early Pleistocene hominin presence at Pirro Nord (Apricena, Foggia, southern Italy):
911 P13 site. Quaternary International 267, 56-61. doi:10.1016/j.quaint.2011.01.042.
912
913 Auguste, P., 1995. Cadres biostratigraphiques et paléoécologiques du peuplement
914 humain dans la France septentrionale durant le Pléistocène: apports de l'étude
915 paléontologique des grands mammifères du gisement de Biache-Saint-Vaast (Pas-
916 de-Calais). Unpublished PhD thesis, Muséum National d'Histoire Naturelle, Paris.
917

918 Behrensmeyer, A.K., 1988. Vertebrate preservation in fluvial channels.
919 Palaeogeography, Palaeoclimatology, Palaeoecology 63, 183-199.
920 doi:10.1016/0031-0182(88)90096-X.
921
922 Bishop, M.J., 1974. A preliminary report on the Middle Pleistocene mammal bearing
923 deposits of Westbury-sub-Mendip, Somerset. Proceedings of the University of Bristol
924 Spelaeological Society 13, 301-318.
925
926 Bishop, M.J., 1975. Earliest record of man's presence in Britain. Nature 253, 95-97.
927 doi:10.1038/253095a0.
928
929 Bishop, M.J., 1982. The mammal fauna of the early Middle Pleistocene cavern infill
930 site of Westbury-sub-Mendip, Somerset. Special Papers in Palaeontology 28, 1-108.
931
932 Blott, S.J., Pye, K., 2001. GRADISTAT: a grain size distribution and statistics
933 package for the analysis of unconsolidated sediments. Earth Surface Processes and
934 Landforms 26, 1237-1248. doi:10.1002/esp.261.
935
936 Bosch, R.F., White, W.B., 2004. Lithofacies and transport of clastic sediments in
937 karstic aquifers. In: Sasowsky, I.D., Mylroie, J.E. (Eds.), Studies of cave sediments.
938 Kluwer Academic/ Plenum Publishers, New York, pp. 1-22. doi:10.1007/978-1-4419-
939 9118-8_1.
940

941 Bridgland, D.R., 1986. Discussion of procedures and recommendations. In:
942 Bridgland, D.R. (Ed.), *Clast lithological analysis*. Technical guide no. 3. Quaternary
943 Research Association, London, pp. 1-33.
944

945 Bridgland, D.R., 1988. The Pleistocene fluvial stratigraphy and palaeogeography of
946 Essex. *Proceedings of the Geologists' Association* 99, 291-314. doi:10.1016/S0016-
947 7878(88)80055-5.
948

949 Butler, R.F., 1992. *Paleomagnetism: magnetic domains to geologic terranes*.
950 Blackwell Scientific, Oxford, pp. 319.
951

952 Carreck, J.N., 1955. The Quaternary vertebrates of Dorset, fossil and sub-fossil.
953 *Proceedings of the Dorset Natural History and Archaeological Society* 75: 164-188.
954

955 Clark, P.U., Archer, D., Pollard, D., Blum, J.D., Rial, J.A., Brovkin, V., Mix, A.C.,
956 Piasias, N.G., Roy, M., 2006. The middle Pleistocene transition: characteristics,
957 mechanisms, and implications for long-term changes in atmospheric pCO₂.
958 *Quaternary Science Reviews* 25, 3150-3184. doi:10.1016/j.quascirev.2006.07.008.
959

960 Coakley, J.P., Syvitski, J.P.M., 1991. SediGraph technique. In: Syvitski, J.P.M. (Ed.),
961 *Principles, methods and applications of particle size analysis*. Cambridge University
962 Press, Cambridge, pp. 129-142.
963

964 Cook, J., 1999. Description and analysis of the flint finds from Westbury Cave. In:
965 Andrews, P., Cook, J., Carrant, A., Stringer, C. (Eds.), *Westbury Cave: The Natural*

966 History Museum excavations 1976-1984. Western Academic & Specialist Press Ltd.,
967 Bristol, pp. 211-262.
968

969 Dawkins, W.B., 1903. On the discovery of an ossiferous cavern of Pliocene age at
970 Dove Holes, Buxton (Derbyshire). *Quarterly Journal of the Geological Society* 59,
971 105-132. doi:10.1144/GSL.JGS.1903.059.01-04.14.
972

973 Dennell, R., Roebroeks, W., 2005. An Asian perspective on early human dispersal
974 from Africa. *Nature* 438, 1099-1104. doi:10.1038/nature04259.
975

976 Donovan, D.T., 1969. Geomorphology and hydrology of the central Mendips,
977 Somerset. *Proceedings of the University of Bristol Speleological Society* 12, 63-74.
978

979 Farrant, A.R., 1995. Long-term Quaternary chronologies from cave deposits.
980 Unpublished PhD thesis, University of Bristol.
981

982 Farrant, A.R., Smart, P.L., 2011. Role of sediment in speleogenesis; sedimentation
983 and paragenesis. *Geomorphology* 134, 79-93. doi:10.1016/j.geomorph.2011.06.006.
984

985 Farrant, A.R., Vranich, R.D., Ensom, P.C., Wilkinson, I.P., Woods, M.A., 2014. New
986 evidence of the Cretaceous overstep of the Mendip Hills, Somerset, UK.
987 *Proceedings of the Geologists' Association* 125, 63-73.
988 doi:10.1016/j.pgeola.2013.08.003.
989

990 Fisher, O., 1877. *Elephas meridionalis* in Dorset. Geological Magazine 4, 527.
991 doi:10.1017/S0016756800150083.
992
993 Fisher, O., 1888. On the occurrence of *Elephas meridionalis* at Dewlish, Dorset.
994 Quarterly Journal of the Geological Society 44, 818-824.
995 doi:10.1144/GSL.JGS.1888.044.01-04.51.
996
997 Fisher, O., 1905. On the occurrence of *Elephas meridionalis* at Dewlish (Dorset).
998 Second communication: human agency suggested. Quarterly Journal of the
999 Geological Society 61, 35-38. doi:10.1144/GSL.JGS.1905.061.01-04.06.
1000
1001 Fisher, O., 1913. The elephant trench at Dewlish—was it dug? Nature 92, 6.
1002 doi:10.1038/092006b0.
1003
1004 Ford, D.C., Stanton, W.I., 1968. The geomorphology of the south-central Mendip
1005 Hills. Proceedings of the Geologists' Association 79, 401-427. doi:10.1016/S0016-
1006 7878(68)80012-4.
1007
1008 Ford, T.D., 2001. Sediments in caves. British Cave Research Association, Buxton,
1009 pp. 32.
1010
1011 Funnell, B.M., 1995. Global sea-level and the (pen-)insularity of late Cenozoic
1012 Britain. Geological Society, London, Special Publications 96, 3-13.
1013 doi:10.1144/GSL.SP.1995.096.01.02.
1014

1015 Funnell, B.M., 1996. Plio-Pleistocene palaeogeography of the southern North Sea
1016 basin (3.75-0.60 Ma). *Quaternary Science Reviews* 15, 391-405. doi:10.1016/0277-
1017 3791(96)00022-4.
1018

1019 Gabunia, L., Vekua, A., Lordkipanidze, D, Swisher, C.C. Ferring, R., Justus, A.,
1020 Nioradze, M., Tvalchrelidze, M., Antón, S.C., Bosinski, G., Jöris, O., de Lumley, M.-
1021 A., Majsuradze, G., Mouskhelishvili, A., 2000. Earliest Pleistocene hominid cranial
1022 remains from Dmanisi, Republic of Georgia: taxonomy, geological setting and age.
1023 *Science* 288, 1019-1025. doi:10.1126/science.288.5468.1019.
1024

1025 Gale, S.J., Hoare, P.G., 1991. *Quaternary sediments: petrographic methods for the*
1026 *study of unlithified rocks*. Belhaven, London, pp. 323.
1027

1028 Gentry, A.W., 1999. Fossil ruminants (Mammalia, Artiodactyla) from Westbury Cave.
1029 In: Andrews, P., Cook, J., Currant, A., Stringer, C. (Eds.), *Westbury Cave: The*
1030 *Natural History Museum excavations 1976-1984*. Western Academic & Specialist
1031 Press Ltd., Bristol, pp. 139-174.
1032

1033 Gibbard, P.L., 1988. The history of the great northwest European rivers during the
1034 past three million years. *Philosophical Transactions of the Royal Society B* 318, 559-
1035 602. doi:10.1098/rstb.1988.0024.
1036

1037 Gibbard, P.L., 2012. The status of the Hill House 'Formation' at Happisburgh,
1038 Norfolk, England. *Quaternary International* 271, 29-30.
1039 doi:10.1016/j.quaint.2011.09.014.

1040

1041 Gibbard, P.L., West, R.G., Zagwijn, W.H., Balson, P.S., Burger, A.W., Funnell, B.M.,
1042 Jeffery, D.H., de Jong, J., van Kolfschoten, T., Lister, A.M., Meijer, T., Norton,
1043 P.E.P., Preece, R.C., Rose, J., Stuart, A.J., Whiteman, C.A., Zalasiewicz, J., 1991.
1044 Early and early Middle Pleistocene correlations in the southern North Sea basin.
1045 Quaternary Science Reviews 10, 23-52. doi:10.1016/0277-3791(91)90029-T.

1046

1047 Gillieson, D., 1986. Cave sedimentation in the New Guinea highlands. Earth Surface
1048 Processes and Landforms 11, 533-543. doi:10.1002/esp.3290110508.

1049

1050 Green, G.W., Welch, F.B.A, 1965. Geology of the country around Wells and Cheddar
1051 (Explanation of One-inch Geological Sheet 280, New Series). Her Majesty's
1052 Stationery Office, London, pp. 225.

1053

1054 Heal, G.J., 1970. A new Pleistocene mammal site, Mendip Hills, Somerset.
1055 Proceedings of the University of Bristol Spelaeological Society 12, 135-136.

1056

1057 Hopson, P.M., Farrant, A.R., Booth, K.A., 2001. Lithostratigraphy and regional
1058 correlation of the basal Chalk, Upper Greensand, Gault, and uppermost Folkestone
1059 formations (Mid-Cretaceous) from cored boreholes near Selborne, Hampshire.
1060 Proceedings of the Geologists' Association 112, 193-210. doi:10.1016/S0016-
1061 7878(01)80001-8.

1062

1063 Huggett, R.J., 2011. Fundamentals of geomorphology. Routledge, London, pp. 516.

1064

1065 Jones, A.P., Tucker, M.E., Hart, J.K., 1999. Guidelines and recommendations. In:
1066 Jones, A.P., Tucker, M.E., Hart, J.K. (Eds.), The description and analysis of
1067 Quaternary stratigraphic field sections. Technical guide no. 7. Quaternary Research
1068 Association, London, pp. 27-76.

1069

1070 Jones, R.L., Keen, D.H., 1993. Pleistocene environments in the British Isles.
1071 Chapman and Hall, London, pp. 346.

1072

1073 Kasse, C., 1990. Lithostratigraphy and provenance of the Early-Pleistocene deposits
1074 in the southern Netherlands and northern Belgium. *Geologie en Mijnbouw* 69, 327-
1075 240.

1076

1077 Kender, S., Ravelo, A.C., Worne, S., Swann, G.E.A., Leng, M.J., Asahi, H., Becker,
1078 J., Detlef, H., Aiello, I.W., Andreasen, D., Hall, I.R., 2018. Closure of the Bering Strait
1079 caused Mid-Pleistocene Transition cooling. *Nature Communications* 9, 5386.
1080 doi:10.1038/s41467-018-07828-0.

1081

1082 Kirschvink, J.L., 1980. The least-squares line and plane and the analysis of
1083 palaeomagnetic data. *Geophysical Journal of the Royal Astronomical Society* 62,
1084 699-718. doi:10.1111/j.1365-246X.1980.tb02601.x.

1085

1086 Lee, J.R., Candy, I., Haslam, R., 2018. The Neogene and Quaternary of England:
1087 landscape evolution, tectonics, climate change and their expression in the geological
1088 record. *Proceedings of the Geologists' Association* 129, 452-481.
1089 doi:10.1016/j.pgeola.2017.10.003.

1090

1091 Lewis, S.G., Maddy, D., Scaife, R.G., 2001. The fluvial system response to abrupt
1092 climate change during the last cold stage: the Upper Pleistocene River Thames
1093 fluvial succession at Ashton Keynes, UK. *Global and Planetary Change* 28, 341-359.
1094 doi:10.1016/S0921-8181(00)00083-7.

1095

1096 Lisiecki, L.E., Raymo, M.E., 2005. A Pliocene-Pleistocene stack of 57 globally
1097 distributed benthic $\delta^{18}\text{O}$ records. *Paleoceanography* 20, PA1003.
1098 doi:10.1029/2004PA001071.

1099

1100 Lordkipanidze, D., Ponce de León, M.S., Margvelashvili, A., Rak, Y., Rightmire, G.P.,
1101 Vekua, A., Zollikofer, C.P.E., 2013. A complete skull from Dmanisi, Georgia, and the
1102 evolutionary biology of early *Homo*. *Science* 342, 326-331.
1103 doi:10.1126/science.1238484.

1104

1105 Martini, I., 2011. Cave clastic sediments and implications for speleogenesis: new
1106 insights from the Mugnano Cave (Montagnola Senese, Northern Apennines, Italy).
1107 *Geomorphology* 134, 452-460. doi:10.1016/j.geomorph.2011.07.024.

1108

1109 Mathers, S.J., Zalasiewicz, J.A., 1988. The Red Crag and Norwich Crag Formations
1110 of southern East Anglia. *Proceedings of the Geologists' Association* 99, 261-278.
1111 doi:10.1016/S0016-7878(97)80002-8.

1112

1113 McClymont, E.L., Sostdian, S.M., Rosell-Melé, A., Rosenthal, Y., 2013. Pleistocene
1114 sea-surface temperature evolution: early cooling, delayed glacial intensification, and

1115 implications for the mid-Pleistocene climate transition. *Earth-Science Reviews* 123,
1116 173-193. doi:10.1016/j.earscirev.2013.04.006.

1117

1118 Meijer, T., 1986. Non-marine biozonation in relation to transgressions in the
1119 Quaternary of the Netherlands. Abstracts of the 9th International Malacological
1120 Congress, Edinburgh, pp. 53.

1121

1122 Michel, V., Shen, C.-C., Woodhead, J., Hu, H.-M., Wu, C.-C., Moullé, P.-É., Khatib,
1123 S., Cauche, D., Moncel, M.-H., Valensi, P., Chou, Y.-M., Gallet, S., Echassoux, A.,
1124 Orange, F., de Lumley, H., 2017. New dating evidence of the early presence of
1125 hominins in southern Europe. *Scientific Reports* 7, 10074. doi:10.1038/s41598-017-
1126 10178-4.

1127

1128 Moriarty, K.C., McCulloch, M.T., Wells, R.T., McDowell, M.C., 2000. Mid-Pleistocene
1129 cave fills, megafaunal remains and climate change at Naracoorte, South Australia:
1130 towards a predictive model using U-Th dating of speleothems. *Palaeogeography,*
1131 *Palaeoclimatology, Palaeoecology* 159, 113-143. doi:10.1016/S0031-
1132 0182(00)00036-5.

1133

1134 Palmer, A.N., 1991. Origin and morphology of limestone caves. *Geological Society*
1135 *of America Bulletin* 103, 1-21. doi:10.1130/0016-
1136 7606(1991)103<0001:OAMOLC>2.3.CO;2.

1137

1138 Parfitt, S.A., Ashton, N.M., Lewis, S.G., Abel, R.L., Coope, G.R., Field, M.H., Gale,
1139 R., Hoare, P.G., Larkin, N.R., Lewis, M.D., Karloukovski, V., Maher, B.A., Peglar,

1140 S.M., Preece, R.C., Whittaker, J.E., Stringer, C., 2010. Early Pleistocene human
1141 occupation at the edge of the boreal zone in northwest Europe. *Nature* 466, 229-233.
1142 doi:10.1038/nature09117.
1143
1144 Pickering, R., Kramers, J.D., 2010. Re-appraisal of the stratigraphy and
1145 determination of new U-Pb dates for the Sterkfontein hominin site, South Africa.
1146 *Journal of Human Evolution* 59, 70-86. doi:10.1016/j.jhevol.2010.03.014.
1147
1148 Pickering, R., Hancox, P.J., Lee-Thorp, J.A., Grün, R., Mortimer, G.E., McCulloch,
1149 M., Berger, L.R., 2007. Stratigraphy, U-Th chronology, and paleoenvironments at
1150 Gladysvale Cave: insights into the climatic control of South African hominin-bearing
1151 cave deposits. *Journal of Human Evolution* 53, 602-619.
1152 doi:10.1016/j.jhevol.2007.02.005.
1153
1154 Pickering, R., Kramers, J.D., Hancox, P.J., de Ruiter, D.J., Woodhead, J.D., 2011.
1155 Contemporary flowstone development links early hominin bearing cave deposits in
1156 South Africa. *Earth and Planetary Science Letters* 306, 23-32.
1157 doi:10.1016/j.epsl.2011.03.019.
1158
1159 Preece, R.C., Parfitt, S.A., 2012. The Early and early Middle Pleistocene context of
1160 human occupation and lowland glaciation in Britain and northern Europe. *Quaternary*
1161 *International* 271, 6-28. doi:10.1016/j.quaint.2012.04.018.
1162

1163 Reid, C., Reid, E.M., 1907. The fossil flora of Tegelen-sur-Meuse, near Venloo, in
1164 the province of Limburg. *Verhandelingen der Koninklijke Akademie van*
1165 *Wetenschappen te Amsterdam, Afdeling Natuurkunde. Tweede sectie* 13, 1-22.
1166

1167 Rose, J., 1994. Major river systems of central and southern Britain during the Early
1168 and Middle Pleistocene. *Terra Nova* 6, 435-443. doi:10.1111/j.1365-
1169 3121.1994.tb00887.x.

1170

1171 Rose, J., 2009. Early and Middle Pleistocene landscapes of eastern England.
1172 *Proceedings of the Geologists' Association* 120, 3-33.
1173 doi:10.1016/j.pgeola.2009.05.003.

1174

1175 Rose, J., Whiteman, C.A., Allen, P., Kemp, R.A., 1999. The Kesgrave Sands and
1176 Gravels: 'pre-glacial' Quaternary deposits of the River Thames in East Anglia and
1177 the Thames valley. *Proceedings of the Geologists' Association* 110, 93-116.
1178 doi:10.1016/S0016-7878(99)80063-7.

1179

1180 Rose, J., Moorlock, B.S.P., Hamblin, R.J.O., 2001. Pre-Anglian fluvial and coastal
1181 deposits in Eastern England: lithostratigraphy and palaeoenvironments. *Quaternary*
1182 *International* 79, 5-22. doi:10.1016/S1040-6182(00)00119-1.

1183

1184 Rose, J., Candy, I., Moorlock, B.S.P., Wilkins, H., Lee, J.A., Hamblin, R.J.O., Lee,
1185 J.R., Riding, J.B., Morigi, A.N., 2002. Early and early Middle Pleistocene river,
1186 coastal and neotectonic processes, southeast Norfolk, England. *Proceedings of the*
1187 *Geologists' Association* 113, 47-67. doi:10.1016/S0016-7878(02)80006-2.

1188

1189 Simms, M.J., 1994. Emplacement and preservation of vertebrates in caves and
1190 fissures. *Zoological Journal of the Linnean Society* 112, 261-283. doi:10.1111/j.1096-
1191 3642.1994.tb00320.x.

1192

1193 Sommé, J., 2013. Unités lithostratigraphiques quaternaires du nord de la France: un
1194 inventaire. *Quaternaire* 24, 3-12. doi:10.4000/quaternaire.6441.

1195

1196 Spencer, H.E.P., Melville, R.V., 1974. The Pleistocene mammalian fauna of Dove
1197 Holes, Derbyshire. *Bulletin of the Geological Survey of Great Britain* 48, 43-49.

1198

1199 Stanton, W.I., 1973. Notes on the geology and geomorphology of the Westbury bone
1200 fissure. *Journal of the Wessex Cave Club* 12, 289-293.

1201

1202 Stanton, W.I., 1999. Early stages in the development of Westbury Cave. In:
1203 Andrews, P., Cook, J., Carrant, A., Stringer, C. (Eds.), *Westbury Cave: The Natural*
1204 *History Museum excavations 1976-1984*. Western Academic and Specialist Press
1205 Limited, Bristol, pp. 13-18.

1206

1207 Stein, R., 1985. Rapid grain-size analyses of clay and silt fraction by SediGraph
1208 5000D: comparison with Coulter counter and Atterberg methods. *Journal of*
1209 *Sedimentary Petrology* 55, 590-593.

1210

1211 Talbot, M.R., Allen, P.A., 1999. Lakes. In: Reading, H.G. (Ed.) *Sedimentary*
1212 *environments: processes, facies and stratigraphy*. Blackwell Science, Oxford, pp. 83-
1213 124.
1214
1215 Toro-Moyano, I., Martínez-Navarro, B., Agustí, J., Souday, C., Bermúdez de Castro,
1216 J.M., Martínón-Torres, M., Fajardo, B., Duval, M., Falguères, C., Oms, O., Parés,
1217 J.M., Anadón, P., Julià, R., García-Aguilar, J.M., Moigne, A.-M., Espigares, M.P.,
1218 Ros-Montoya, S., Palmqvist, P., 2013. The oldest human fossil in Europe, from Orce
1219 (Spain). *Journal of Human Evolution* 65, 1-9. doi:10.1016/j.jhevol.2013.01.012.
1220
1221 van den Hoek Ostende, L.W., 2004. The Tegelen clay-pits: a hundred year old
1222 classical locality. *Scripta Geologica, Special Issue 4*, 127-141.
1223
1224 Van Gundy, J.J., White, W.B., 2009. Sediment flushing in Mystic Cave, West
1225 Virginia, USA, in response to the 1985 Potomac Valley flood. *International Journal of*
1226 *Speleology* 38, 103-109. doi:10.5038/1827-806X.38.2.2.
1227
1228 Vandenberghe, J., Kasse, C., 1989. Periglacial environments during the early
1229 Pleistocene in the southern Netherlands and northern Belgium. *Palaeogeography,*
1230 *Palaeoclimatology, Palaeoecology* 72, 133-139. doi:10.1016/0031-0182(89)90137-5.
1231
1232 Verosub, K.L., 1977. Depositional and postdepositional processes in the
1233 magnetization of sediments. *Reviews of Geophysics and Space Physics* 15, 129–
1234 143. doi:10.1029/RG015i002p00129.
1235

1236 Verosub, K.L., Ensley, R.A., Ulrick, J.S., 1979. The role of water content in the
1237 magnetization of sediments. *Geophysical Research Letters* 6, 226–228.
1238 doi:10.1029/GL006i004p00226.
1239
1240 Villa, A., Blain, H.-A., van den Hoek Ostende, L.W., Delfino, M., 2018. Fossil
1241 amphibians and reptiles from Tegelen (Province of Limburg) and the early
1242 Pleistocene palaeoclimate of the Netherlands. *Quaternary Science Reviews* 187,
1243 203-219. doi:10.1016/j.quascirev.2018.03.020.
1244
1245 West, R.G., 1962. Vegetational history of the Early Pleistocene of the Royal Society
1246 borehole at Ludham, Norfolk. *Proceedings of the Royal Society B* 155, 437-453.
1247 doi:10.1098/rspb.1962.0011.
1248
1249 West, R.G., 1980. Pleistocene forest history in East Anglia. *New Phytologist* 85, 571-
1250 622. doi:10.1111/j.1469-8137.1980.tb00772.x.
1251
1252 Westaway, R., 2009. Quaternary vertical crustal motion and drainage evolution in
1253 East Anglia and adjoining parts of southern England: chronology of the Ingham River
1254 terrace deposits. *Boreas* 38, 261-284. doi:10.1111/j.1502-3885.2008.00068.x.
1255
1256 Westaway, R., 2011. A re-evaluation of the timing of the earliest reported human
1257 occupation of Britain: the age of the sediments at Happisburgh, eastern England.
1258 *Proceedings of the Geologists' Association* 122, 383-396.
1259 doi:10.1016/j.pgeola.2011.03.002.
1260

1261 Westaway, R., Maddy, D., Bridgland, D., 2002. Flow in the lower continental crust as
1262 a mechanism for the Quaternary uplift of south-east England: constraints from the
1263 Thames terrace record. *Quaternary Science Reviews* 21, 559-603.
1264 doi:10.1016/S0277-3791(01)00040-3.
1265
1266 White, W.B., 2007. Cave sediments and paleoclimate. *Journal of Cave and Karst*
1267 *Studies* 69, 76-93.
1268
1269 White, W.B., 2012. Entrances. In: White, W.B., Culver, D.C. (Eds.) *Encyclopedia of*
1270 *caves*. Academic Press, Cambridge, pp. 280-284. doi:10.1016/B978-0-12-383832-
1271 2.00037-2.
1272
1273 Whiteman, C.A., 1992. The palaeogeography and correlation of pre-Anglian-
1274 Glaciation terraces of the River Thames in Essex and the London Basin.
1275 *Proceedings of the Geologists' Association* 103, 37-56. doi:10.1016/S0016-
1276 7878(08)80197-6.
1277
1278 Yassi, N.B.H., 1983. Archaeomagnetic work in Britain and Iraq. Unpublished PhD
1279 thesis, University of Newcastle upon Tyne.
1280
1281 Zagwijn, W.H., 1957. Vegetation, climate and time-correlations in the Early
1282 Pleistocene of Europe. *Geologie en Mijnbouw* 19, 233-244.
1283
1284 Zagwijn, W.H., 1985. An outline of the Quaternary stratigraphy of the Netherlands.
1285 *Geologie en Mijnbouw* 64, 17-24.

1286

1287 Zhu, R.X., Potts, R., Pan, Y.X., Yao, H.T., Lü, L.Q., Zhao, X., Gao, X., Chen, L.W.,

1288 Gao, F., Deng, C.L., 2008. Early evidence of the genus *Homo* in East Asia. *Journal*

1289 of Human Evolution 55, 1075-1085. doi:10.1016/j.jhevol.2008.08.005.

1290 **Figures captions**

1291 Figure 1. The stacked marine oxygen isotope record, LR04 (Lisiecki and Raymo,
1292 2005), for the latest Pliocene, Early Pleistocene, and earliest Middle Pleistocene
1293 (Mid. Pl.), showing the temporal coverage of the Crag Basin sediments (upper grey
1294 bars) and terrestrial fluvial deposits (bottom black bars) in Britain. The possible age
1295 of the Siliceous Member in Westbury Cave from available bio- and
1296 magnetostratigraphy is indicated (dashed boxes). Biostratigraphy by Bishop (1982)
1297 and Gentry (1999) suggests the 1.06-1.78 Ma interval (shown as SM?) might be
1298 more likely than the 0.78-0.91 Ma interval (shown as SM??). The geomagnetic
1299 polarity timescale for LR04 (Cande and Kent, 1995) is shown immediately below the
1300 x-axis; black bars indicate normal polarity, white bars indicate reversed polarity. The
1301 mid-Pleistocene revolution (MPR) is highlighted with a light grey box from 1.25-0.70
1302 Ma (Clark *et al.*, 2006) and approximate timings of key archaeological events are
1303 marked with arrows (see citations in main text).

1304

1305 Figure 2. Location of Westbury Cave in the southwest of the UK (top left) and on the
1306 southern flanks of the Mendip Hills (bottom left). The location of the nearest outcrop
1307 of the Upper Greensand Formation at Tadhil is also shown (bottom left). Right panel
1308 shows detail of Westbury Quarry (also known as Broadmead Quarry); the location of
1309 the studied sections through the Westbury Cave infill is highlighted with a star within
1310 the Brimble Pit and Cross Swallet Basins Site of Special Scientific Interest (SSSI, in
1311 grey with dashed outline). The underlying geology (see coloured key) and
1312 topography (orange contours) are also indicated.

1313

1314 Figure 3. Summary map showing the geology of the Mendip Hills and surrounding
1315 areas. Westbury Cave is shown with a yellow star, and the nearest outliers of the
1316 Cretaceous Upper Greensand Formation at Tadhil and Postlebury Hill (see Farrant
1317 et al., 2014) are shown with green circles. Reproduced from the BGS Geology 625k
1318 dataset (DiGMapGB-625), with the permission of the British Geological Survey
1319 ©UKRI. All rights reserved. Abbreviations: C – Carboniferous, P – Permian, Tr –
1320 Triassic, J – Jurassic, Fm(s) – formation(s), sst – sandstone, cgl – conglomerate, hal
1321 – halite, mdst – mudstone, sltst – siltstone.

1322

1323 Figure 4. Location of the field sections studied through the Siliceous Member
1324 deposits in Westbury Cave on the northeast edge of Westbury Quarry. Areas of *in*
1325 *situ* early Middle Pleistocene Calcareous Member breccia are shown above. Section
1326 1b contains a contact between the Siliceous and Calcareous Members, but
1327 limestone scree slopes and slumped material above and to the side of the Siliceous
1328 Member sections meant extensive exposures of this contact could not be revealed.
1329 Inset photograph shows detail and face relationships through Section 1a.

1330

1331 Figure 5. Section drawings (a-f) and photographs (g-k) of the sediments through
1332 Face 1 to Face 6 of Section 1a, showing sampling locations for palaeomagnetic
1333 dating, particle size analysis, and clast lithology analysis. Main depositional units are
1334 identified with face and unit numbers (e.g., F1U1). Symbols showing samples for
1335 palaeomagnetic dating with emboldened borders indicate the samples that have
1336 results displayed in Figure 9.

1337

1338

1339 Figure 6. Section drawings (a-b) and photographs (c-d) of the sediments connecting
1340 Face 1 of Section 1a with Face 1 of Section 1b. The Calcareous Member breccia is
1341 clearly exposed on the right side of S1b F1 (b, d), but the main contact with the
1342 Siliceous Member is poorly exposed due to slumped material. Main depositional
1343 units are identified with face and unit numbers (e.g., F1U1).

1344

1345 Figure 7. Section drawings (a-c) and photographs (d-e) of the sediments connecting
1346 Faces 1-2 of Section 1c (a-b) with Face 5 of Section 1a (c). Main depositional units
1347 are identified with face and unit numbers (e.g., F1U1).

1348

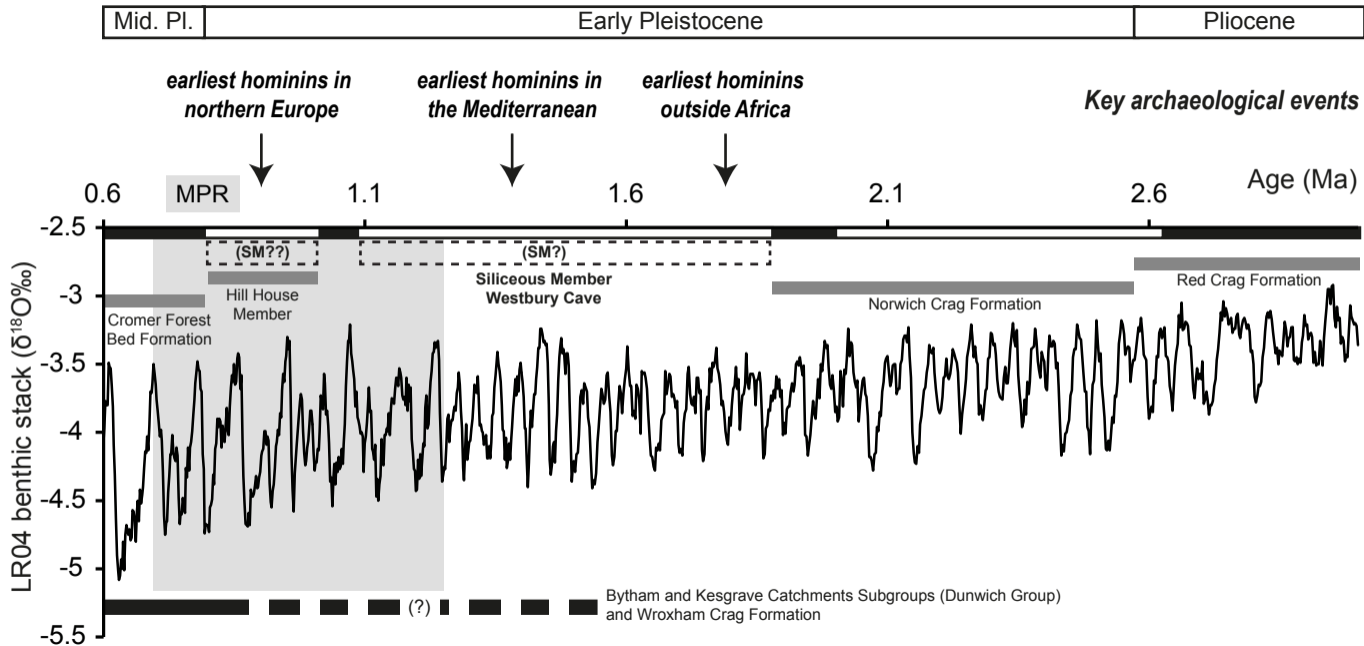
1349 Figure 8. Stratigraphical logs of Sections 1a, 1b, 1c and 2 through the Siliceous
1350 Member in Westbury Cave, showing correlations between them (dashed lines).
1351 Facies associations described in Table 1 are labelled against units along with
1352 sampling locations. The contact between the Calcareous and Siliceous Members is
1353 shown in Section 1b. Main depositional units are identified with face and unit
1354 numbers (e.g., F1U1). Symbols showing samples for palaeomagnetic dating with
1355 emboldened borders indicate the samples that have results displayed in Figure 9.

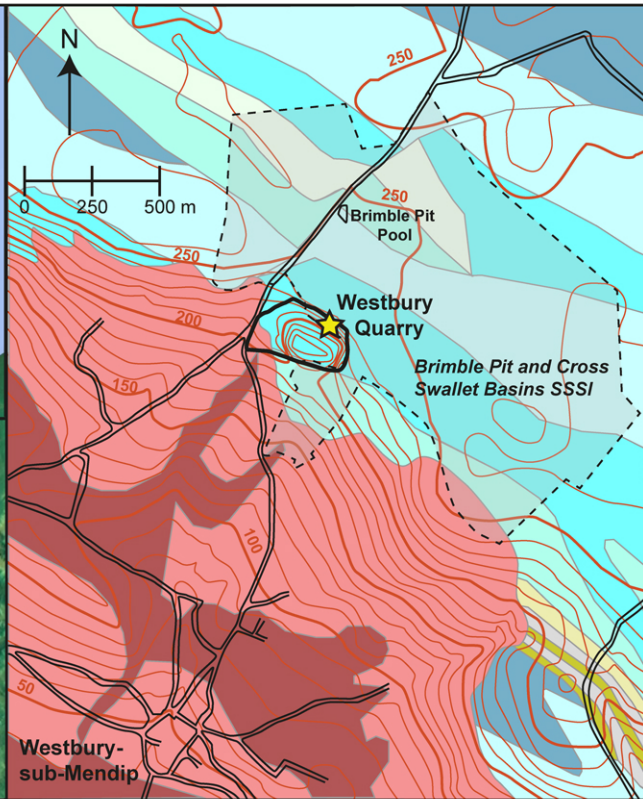
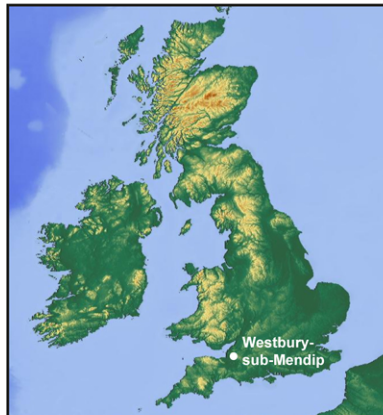
1356

1357 Figure 9. (a) Field sampling of a unit of fine-grained lacustrine sediment for
1358 palaeomagnetic dating. (b-f) Representative orthogonal plots and equal area
1359 stereographic projections obtained from stepwise alternating field demagnetisation of
1360 natural remanent magnetisation of facies association A sediments from each of the
1361 units listed in Table 3. Open and closed circles on orthogonal plots represent vertical
1362 and horizontal planes, respectively. Open circles on stereographic plots are upper
1363 hemisphere projections.

1364

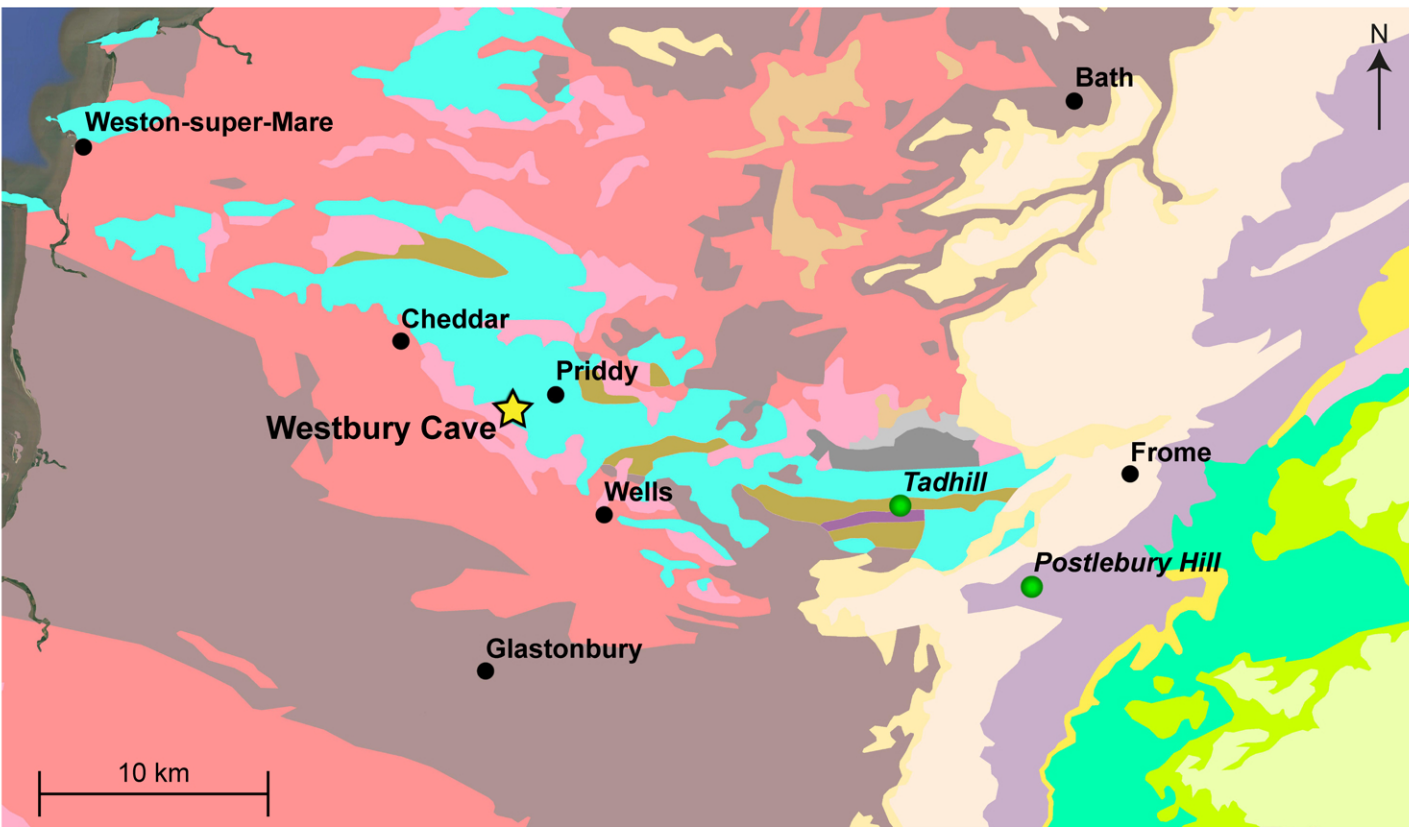
1365 Figure 10. (a) Stereographic plot of all coherent and PCA-fitted sample directions,
1366 and (b) stereographic plots of sample directions for facies association A sediments
1367 from the first five faces (F1-F5) in S1a (see Fig. 5). Directional means and circles of
1368 confidence (α_{95}) are plotted and values listed in Table 3. Means of all samples are
1369 shown by larger grey circles, (b) shows means of each face. Geocentric axial dipole
1370 (GAD) position for a reversed field at sampling latitude (51.25°N) and present Earth's
1371 field (PEF; declination of 2°W, inclination of 66°N) are also plotted.





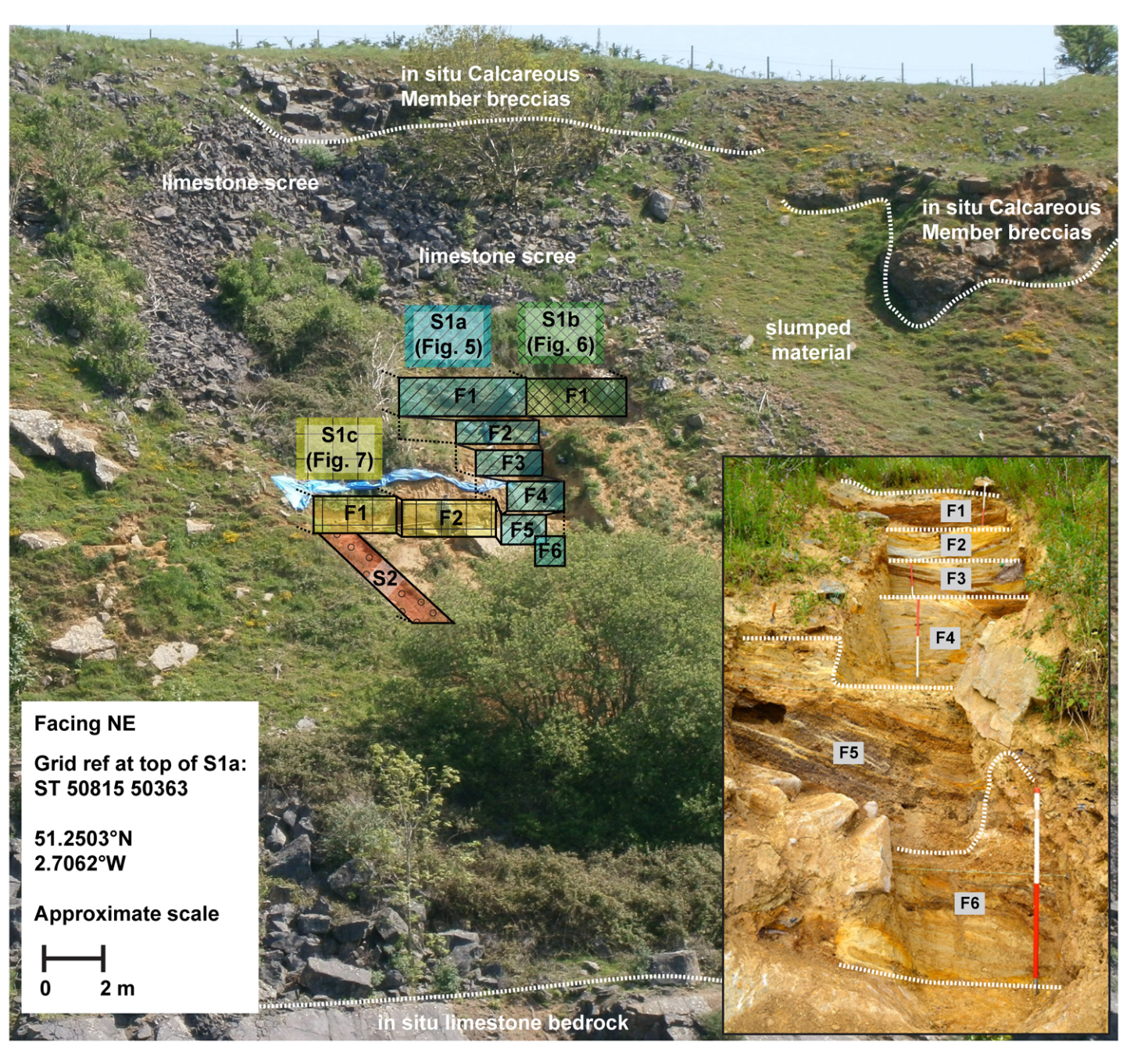
Key to geology

Triassic		mudstone & halite	} Mercia Mudstone Group
		dolomitic conglomerate	
Carboniferous		mud-, silt-, sandstones	} South Wales Lower Coal Measures Fm
		sandstone	
		Quartzitic Sandstone Fm	
		Oxwich Head Limestone Fm	
		"Chinastones" - calcitic mudstone	
		Clifton Down Limestone Fm	
		Burrington Oolite Subgroup	
		Black Rock Limestone Subgroup	



Cretaceous		White Chalk Subgroup
		Grey Chalk Subgroup
		Gault & Upper Greensand Fms
Jurassic		West Walton, Ampthill Clay, Kimmeridge Clay Fms
		Corallian Group
		Kellaways & Oxford Clay Fms
		Great Oolite Group
		Inferior Oolite Group
		Lias Group

Triassic		Mercia Mudstone Group (hal/mdst/sltst/sst)
		Mercia Mudstone Group (dolomitic cgl/sst)
C/P		Warwickshire Group
Carboniferous		Pennine & South Wales Middle Coal Measures Fms
		Pennine & South Wales Lower Coal Measures Fms
		Limestone (minor sst & argillaceous rocks)
Devonian		Portishead Fm
Silurian		Coalbrookdale Fm



in situ Calcareous Member breccias

limestone scree

limestone scree

in situ Calcareous Member breccias

slumped material

S1a
(Fig. 5)

S1b
(Fig. 6)

S1c
(Fig. 7)

F1

F1

F2

F3

F4

F1

F2

F5

F6

S2

F1

F2

F3

F4

F5

F6

Facing NE

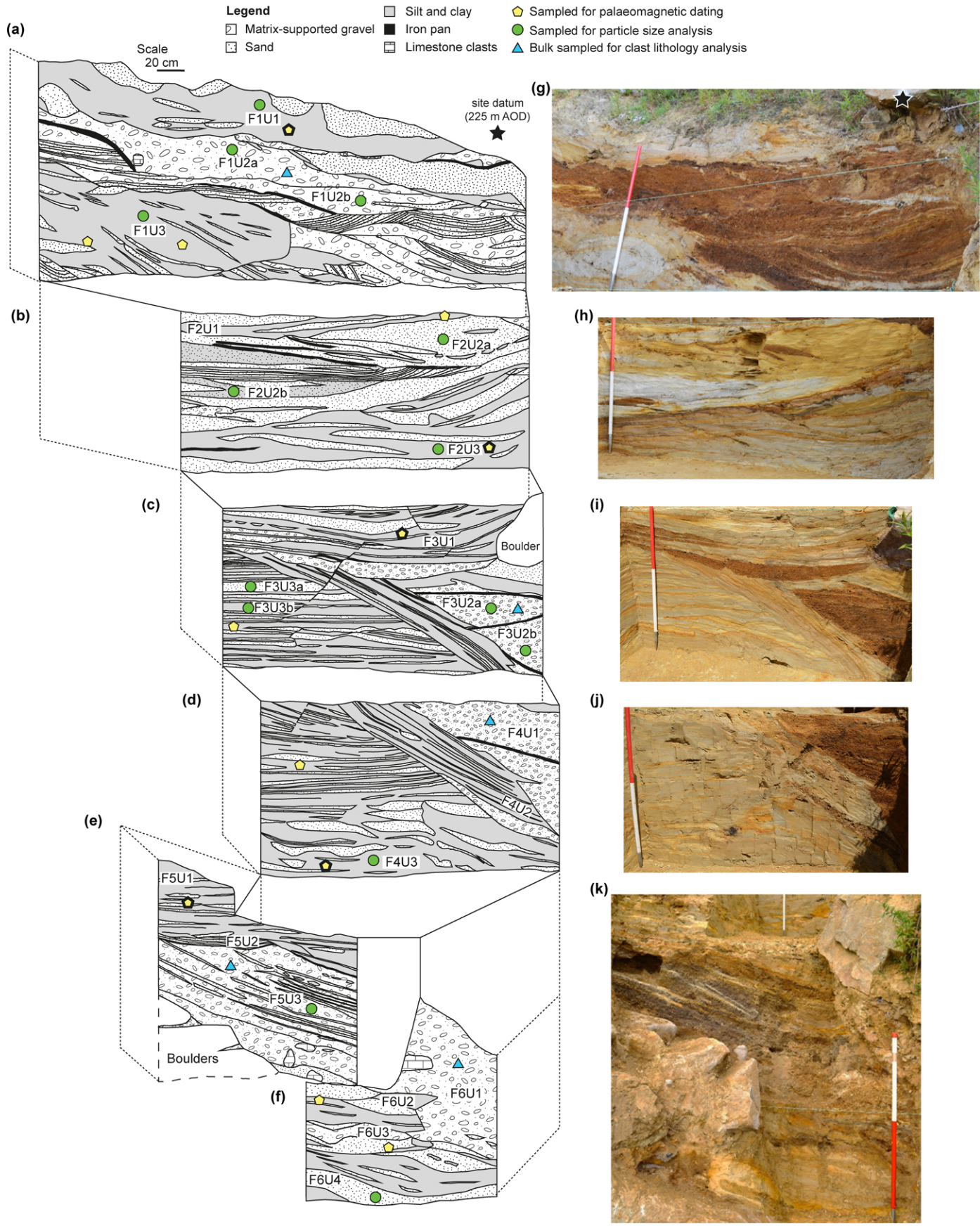
Grid ref at top of S1a:
ST 50815 50363

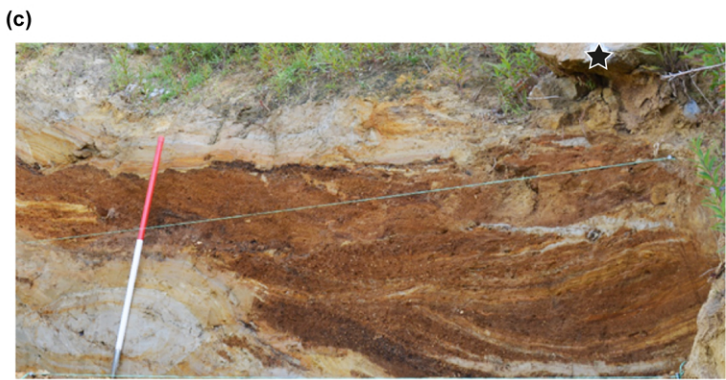
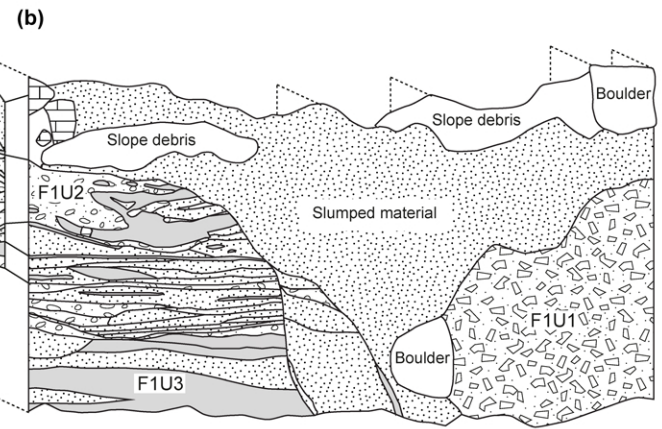
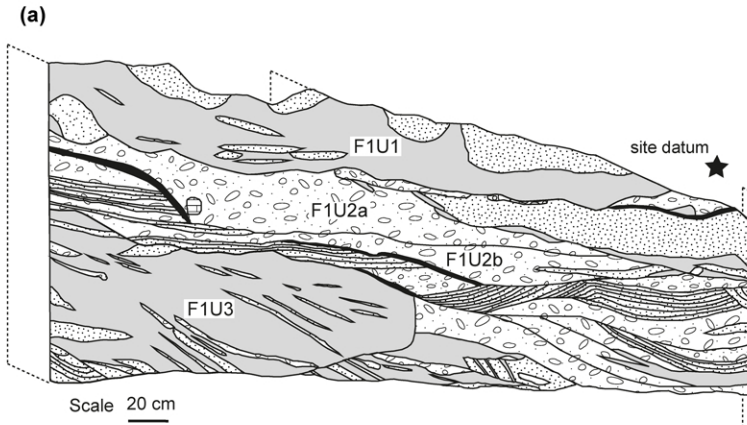
51.2503°N
2.7062°W

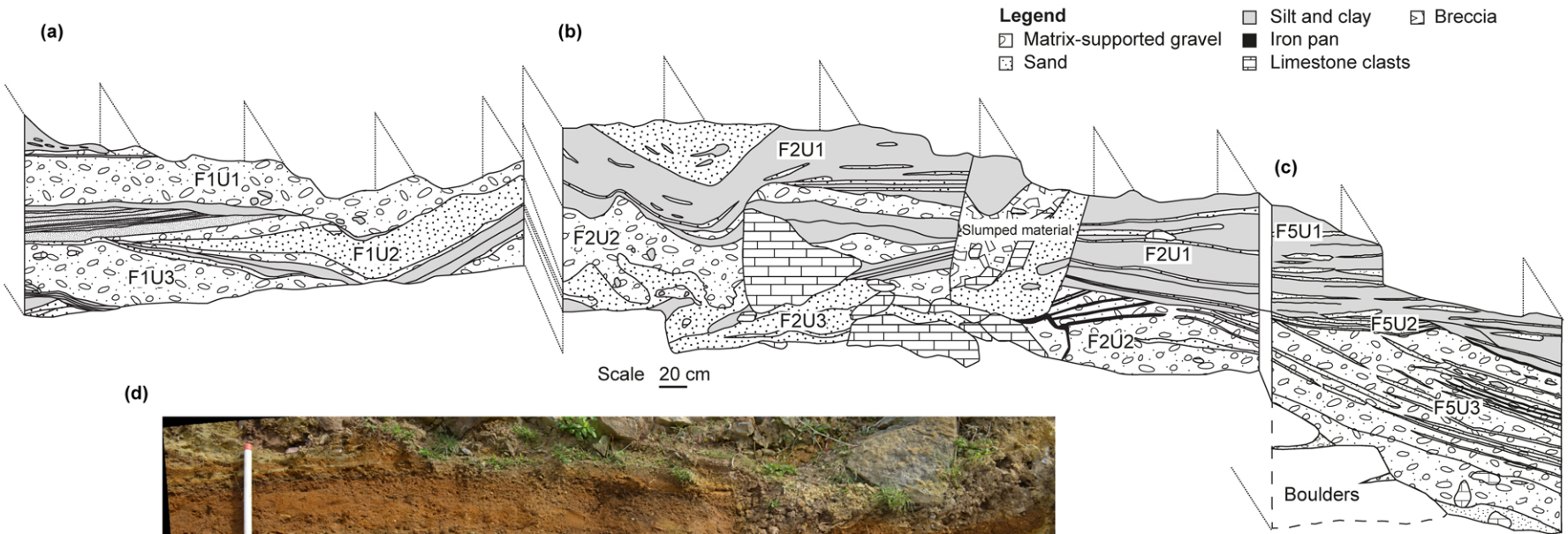
Approximate scale

0 2 m




in situ limestone bedrock







Location of samples for:

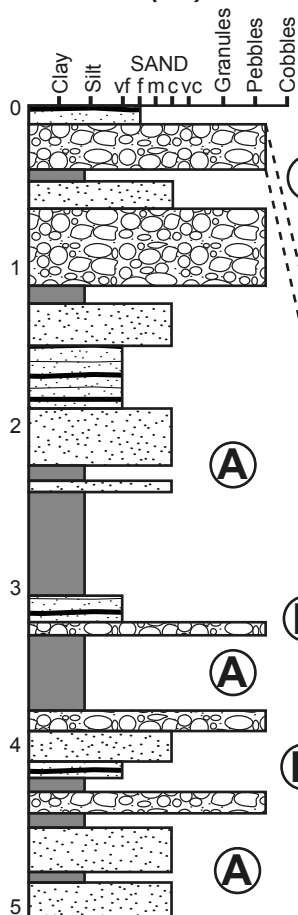
-  Palaeomagnetic dating
-  Particle size analysis
-  Clast lithology analysis

(A) Facies Associations

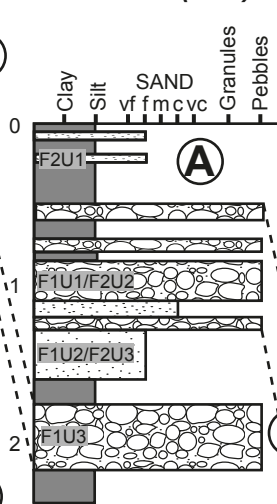
- (B)**
- (C)**
- (D)**
- (E)**

West

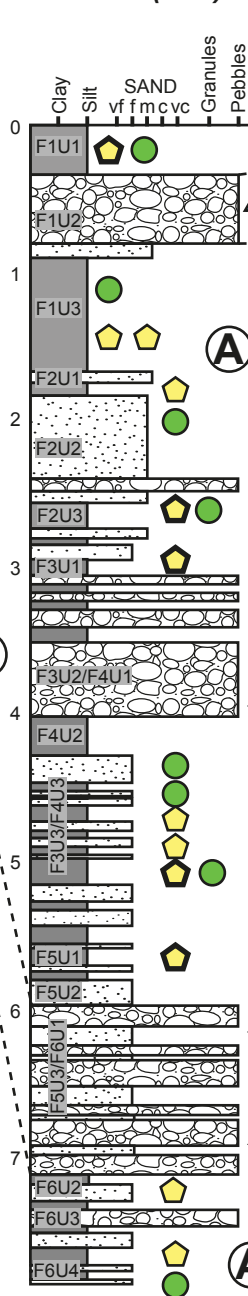
Section 2 (S2)



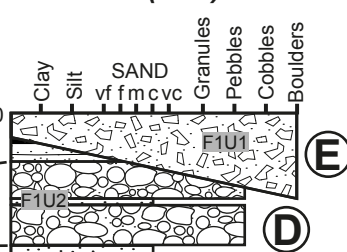
Section 1c (S1c)



Section 1a (S1a)




Section 1b (S1b)




East

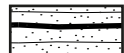
Key

Calcareous Member


 Boulder/cobble limestone breccia

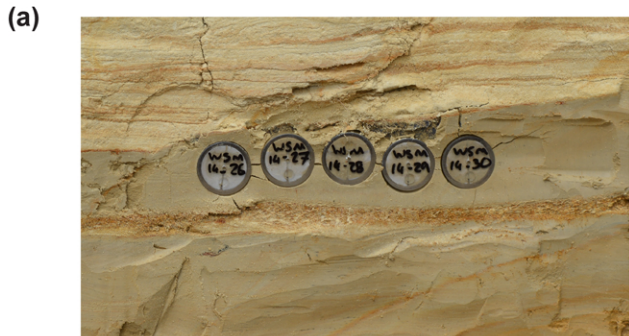
Siliceous Member

 Massive to weakly laminated silts & clays

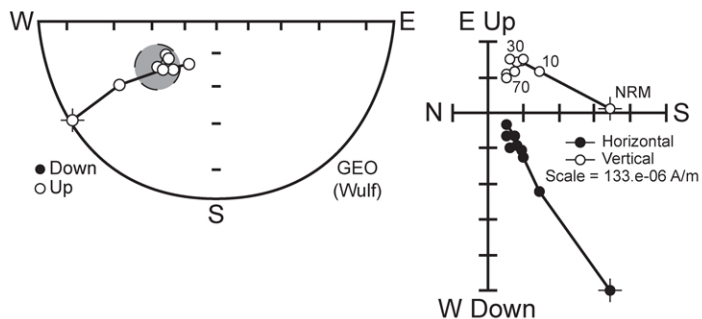
 Laminated sands and silts

 Sands

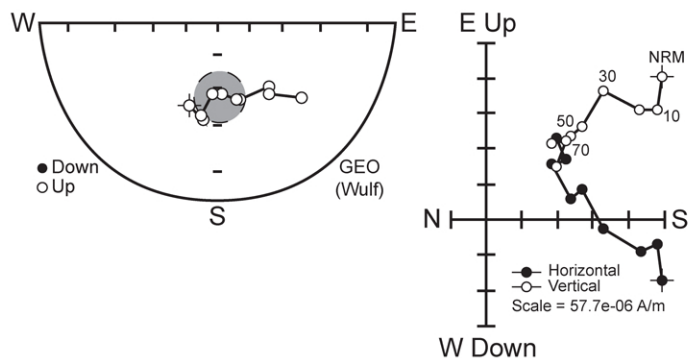
 Pebble dominated gravels



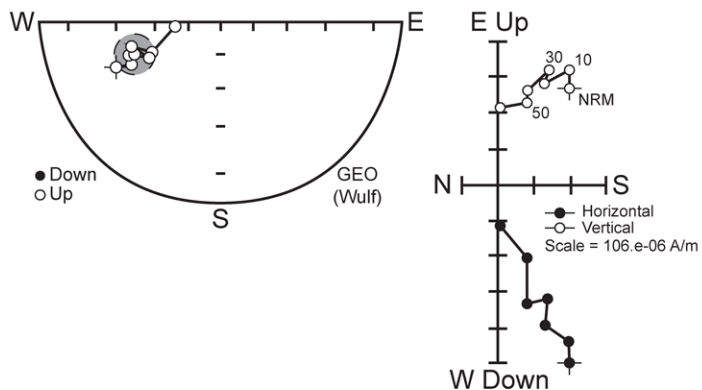
(b) S1a F1U1



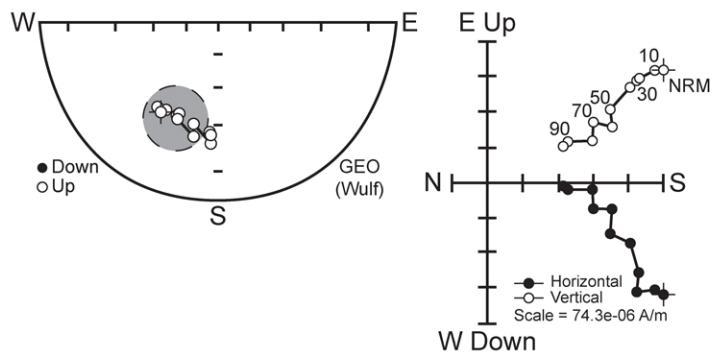
(c) S1a F2U3



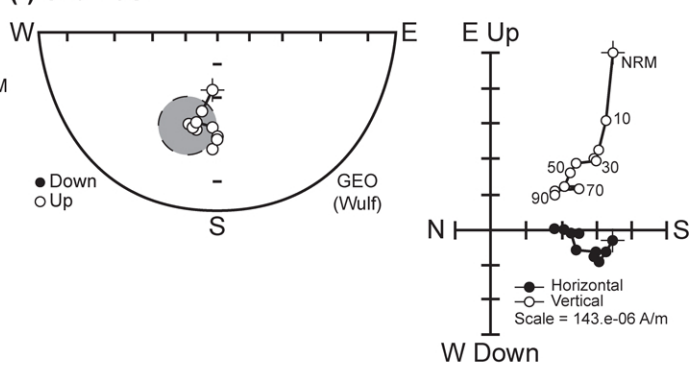
(d) S1a F3U1

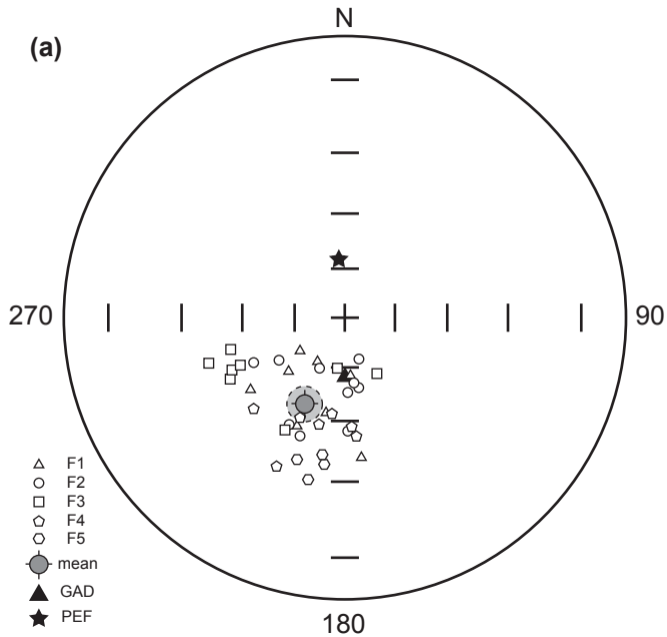
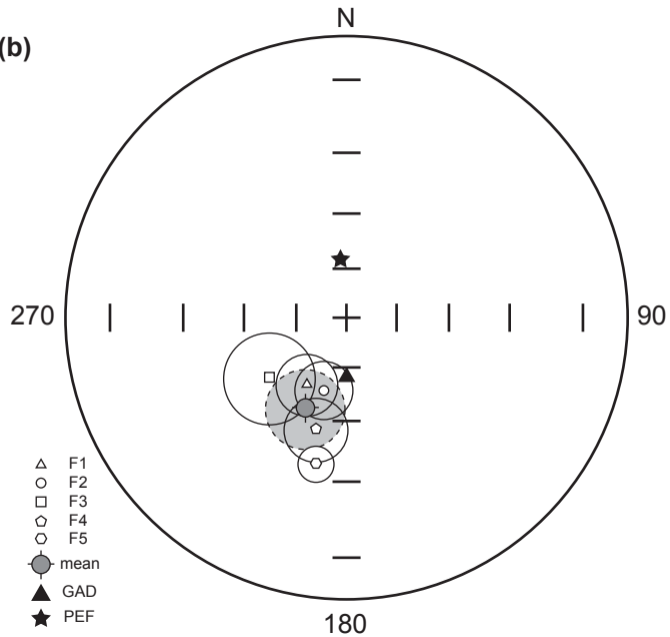


(e) S1a F4U3



(f) S1a F5U1



(a)**(b)**

Supplementary material for:

**Deposition and provenance of the Early Pleistocene Siliceous Member in
Westbury Cave, Somerset, England**

Neil F. Adams, Ian Candy, Danielle C. Schreve, René W. Barendregt

Contents

Figure S1.....	2
Figure S2.....	3
Figure S3.....	4



Figure S1. The current exposure of the Pleistocene cave infill (solid black box) and the Siliceous Member exposures examined in this study (dashed black box), within the surrounding Carboniferous limestone at Westbury Quarry, facing NE (photograph: N.F. Adams).



Fig. S2. The dipping surfaces of sediments ($38-44^{\circ}\text{SE}$) perpendicular to Face 3, revealed during excavation to expose the faces. The base of the dipping sediments is at 318 cm below datum (B.D.). Photograph taken facing 098° (photograph: N.F. Adams, 21 June 2014).

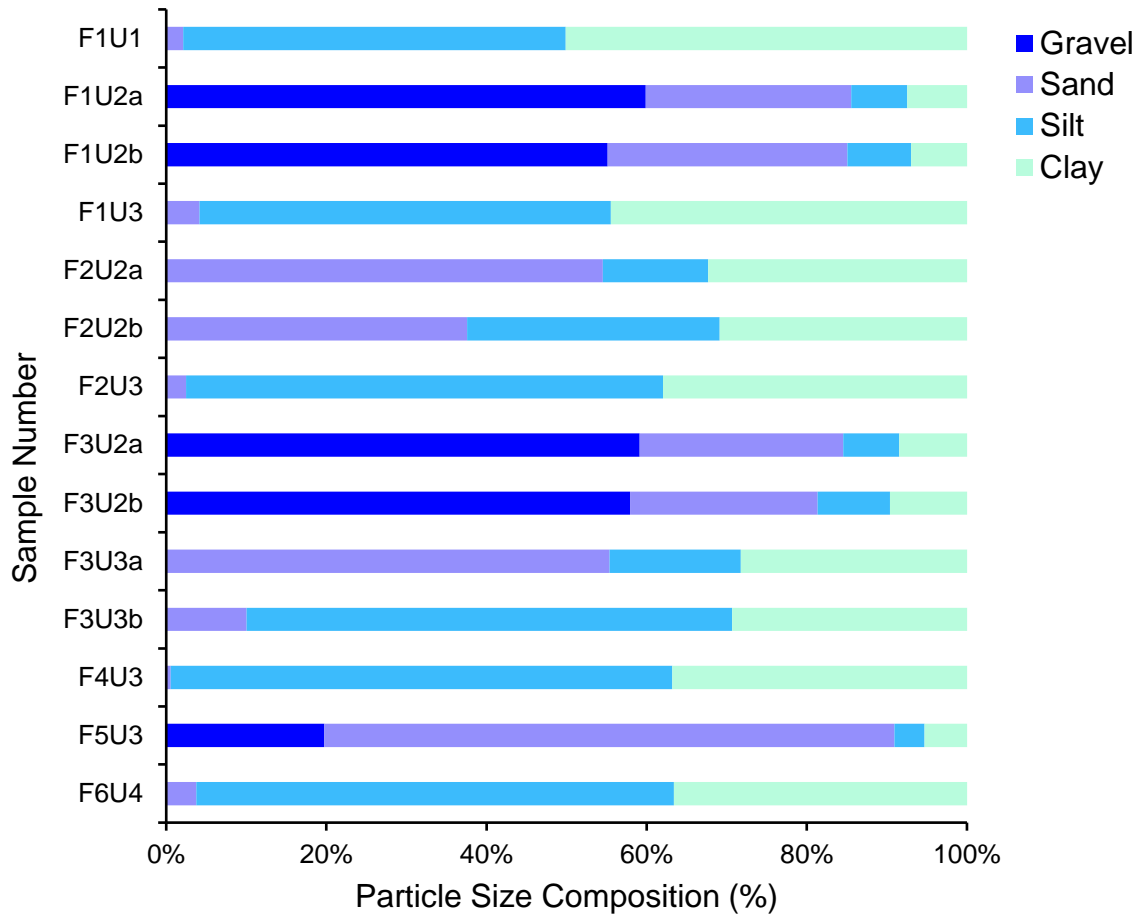


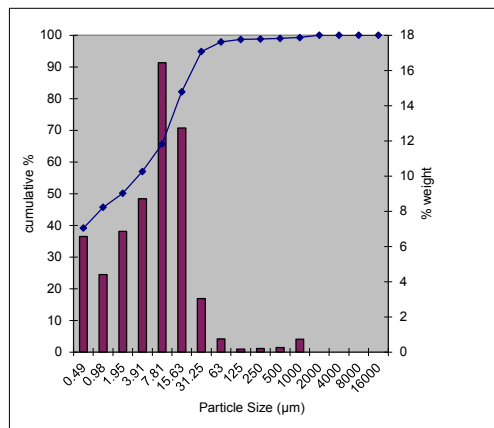
Fig. S3. Particle size distributions for sampled units shown in stratigraphic order from top of the sequence to the bottom.

PARTICLE SIZE ANALYSIS				
LAB. No:	4549	UNIT	FIUI	
LOCATION:	Westbury			
SIEVING RESULTS				
SAMPLE Wt:	30.42			
PHI SIZE:		% TOTAL WEIGHT	% TOTAL PASSING	
GRAVEL				
-6	Res Wt On 64mm Sieve:	0.00	0.00	100.00
-5	Res Wt On 32mm Sieve:	0.00	0.00	100.00
-4	Res Wt On 16mm Sieve:	0.00	0.00	100.00
-3	Res Wt On 8mm Sieve:	0.00	0.00	100.00
-2	Res Wt On 4mm Sieve:	0.00	0.00	100.00
-1	Res Wt On 2mm Sieve:	0.00	0.00	100.00
GRAVEL WT RETAINED:		0.00		
TOTAL WT < 2mm:		30.42		
SAND				
0	Res Wt On 1mm Sieve:	0.22	SAND % 0.72	99.28
1	Res Wt On 500um Sieve:	0.08	0.26	99.01
2	Res Wt On 250um Sieve:	0.06	0.20	98.82
3	Res Wt On 125um Sieve:	0.05	0.16	98.65
4	Res Wt On 63um Sieve:	0.23	0.76	97.90
SAND WT RETAINED:		0.64		
TOTAL WT < 4 PHI:		29.78		

SEDIGRAPH RESULTS				
PHI SIZE:		RETAINED %	% TOTAL WEIGHT	% TOTAL PASSING
5.00	31.25um	3.10	3.03	94.86
6.00	15.63um	13.00	12.73	82.13
7.00	7.81um	16.80	16.45	65.69
8.00	3.91um	8.90	8.71	56.98
9.00	1.95um	7.00	6.85	50.12
10.00	0.98um	4.50	4.41	45.72
11.00	0.49um	6.70	6.56	39.16

TOTAL PERCENTAGES	
% GRAVEL:	0.00
% SAND:	2.10
% SILT	47.77
% CLAY:	50.12
% F CLAY:	39.16

SIZE	% WEIGHT	CUM %
64000mm	0.00	100.00
32000um	0.00	100.00
16000	0.00	100.00
8000	0.00	100.00
4000	0.00	100.00
2000	0.00	100.00
1000	0.72	99.28
500	0.26	99.01
250	0.20	98.82
125	0.16	98.65
63	0.76	97.90
31.25	3.03	94.86
15.63	12.73	82.13
7.81	16.45	65.69
3.91	8.71	56.98
1.95	6.85	50.12
0.98	4.41	45.72
0.49	6.56	39.16
SUM	43.02	

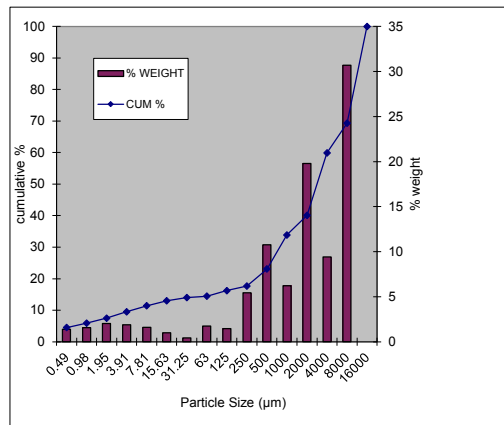


PARTICLE SIZE ANALYSIS				
LAB. No:	4547	UNIT	FIU2 a	
LOCATION:	Westbury			
SIEVING RESULTS				
SAMPLE Wt:	202.00			
PHI SIZE:		% TOTAL WEIGHT	% TOTAL PASSING	
GRAVEL				
-6	Res Wt On 64mm Sieve:	0.00	0.00	100.00
-5	Res Wt On 32mm Sieve:	0.00	0.00	100.00
-4	Res Wt On 16mm Sieve:	0.00	0.00	100.00
-3	Res Wt On 8mm Sieve:	62.00	30.69	69.31
-2	Res Wt On 4mm Sieve:	19.00	9.41	59.90
-1	Res Wt On 2mm Sieve:	40.00	19.80	40.10
GRAVEL WT RETAINED:		121.00		
TOTAL WT < 2mm:		114.22		
SAND				
0	Res Wt On 1mm Sieve:	17.75	SAND % 15.54	6.23
1	Res Wt On 500um Sieve:	30.71	26.89	10.78
2	Res Wt On 250um Sieve:	15.48	13.55	5.43
3	Res Wt On 125um Sieve:	4.11	3.60	1.44
4	Res Wt On 63um Sieve:	5.00	4.38	1.76
SAND WT RETAINED:		73.05		
TOTAL WT < 4 PHI:		29.20		

SEDIGRAPH RESULTS				
PHI SIZE:		RETAINED %	% TOTAL WEIGHT	% TOTAL PASSING
5.00	31.25um	3.00	0.43	14.02
6.00	15.63um	7.00	1.01	13.01
7.00	7.81um	11.10	1.60	11.40
8.00	3.91um	13.10	1.89	9.51
9.00	1.95um	14.10	2.04	7.47
10.00	0.98um	10.90	1.58	5.90
11.00	0.49um	9.60	1.39	4.51

TOTAL PERCENTAGES	
% GRAVEL:	59.90
% SAND:	25.65
% SILT	6.98
% CLAY:	7.47
% F CLAY:	4.51

SIZE	% WEIGHT	CUM %
16000	0.00	100.00
8000	30.69	69.31
4000	9.41	59.90
2000	19.80	40.10
1000	6.23	33.87
500	10.78	23.09
250	5.43	17.65
125	1.44	16.21
63	1.76	14.45
31.25	0.43	14.02
15.63	1.01	13.01
7.81	1.60	11.40
3.91	1.89	9.51
1.95	2.04	7.47
0.98	1.58	5.90
0.49	1.39	4.51
SUM	90.49	

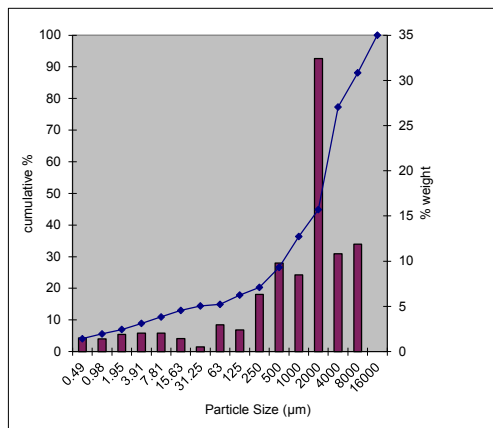


PARTICLE SIZE ANALYSIS				
LAB. No:	4548	UNIT	FIU2 b	
LOCATION:	Westbury			
SIEVING RESULTS				
SAMPLE Wt:	185.00			
PHI SIZE:			% TOTAL WEIGHT	% TOTAL PASSING
GRAVEL				
-6	Res Wt On 64mm Sieve:	0.00	0.00	100.00
-5	Res Wt On 32mm Sieve:	0.00	0.00	100.00
-4	Res Wt On 16mm Sieve:	0.00	0.00	100.00
-3	Res Wt On 8mm Sieve:	22.00	11.89	88.11
-2	Res Wt On 4mm Sieve:	20.00	10.81	77.30
-1	Res Wt On 2mm Sieve:	60.00	32.43	44.86
GRAVEL WT RETAINED:		102.00		
TOTAL WT < 2mm:		110.59		
SAND				
0	Res Wt On 1mm Sieve:	20.92	SAND %	
			18.92	8.49
1	Res Wt On 500um Sieve:	24.11	21.80	9.78
				26.60
2	Res Wt On 250um Sieve:	15.58	14.09	6.32
				20.28
3	Res Wt On 125um Sieve:	5.89	5.33	2.39
				17.89
4	Res Wt On 63um Sieve:	7.28	6.58	2.95
				14.93
SAND WT RETAINED:		73.78		
TOTAL WT < 4 PHI:		27.63		

SEDIGRAPH RESULTS				
PHI SIZE:		RETAINED %	% TOTAL WEIGHT	% TOTAL PASSING
5.00	31.25um	3.40	0.51	14.43
6.00	15.63um	9.60	1.43	12.99
7.00	7.81um	13.70	2.05	10.95
8.00	3.91um	13.70	2.05	8.90
9.00	1.95um	12.80	1.91	6.99
10.00	0.98um	9.30	1.39	5.60
11.00	0.49um	10.20	1.52	4.08

TOTAL PERCENTAGES	
% GRAVEL:	55.14
% SAND:	29.93
% SILT	7.94
% CLAY:	6.99
% F CLAY:	4.08

SIZE	% WEIGHT	CUM %
64000mm	0.00	100.00
32000um	0.00	100.00
16000	0.00	100.00
8000	11.89	88.11
4000	10.81	77.30
2000	32.43	44.86
1000	8.49	36.38
500	9.78	26.60
250	6.32	20.28
125	2.39	17.89
63	2.95	14.93
31.25	0.51	14.43
15.63	1.43	12.99
7.81	2.05	10.95
3.91	2.05	8.90
1.95	1.91	6.99
0.98	1.39	5.60
0.49	1.52	4.08
SUM	91.10	

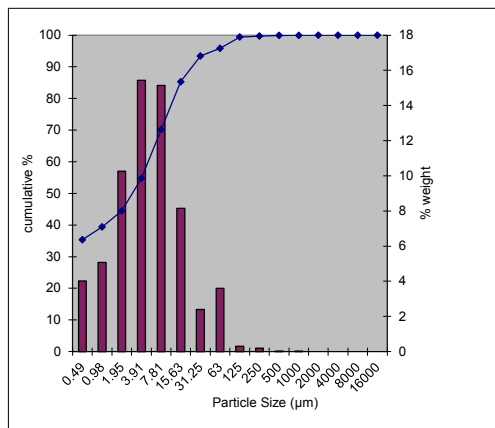


PARTICLE SIZE ANALYSIS				
LAB. No:	4550	UNIT	FIU3	
LOCATION:	Westbury			
SIEVING RESULTS				
SAMPLE Wt:	30.32			
PHI SIZE:		% TOTAL WEIGHT	% TOTAL PASSING	
GRAVEL				
-6	Res Wt On 64mm Sieve:	0.00	0.00	100.00
-5	Res Wt On 32mm Sieve:	0.00	0.00	100.00
-4	Res Wt On 16mm Sieve:	0.00	0.00	100.00
-3	Res Wt On 8mm Sieve:	0.00	0.00	100.00
-2	Res Wt On 4mm Sieve:	0.00	0.00	100.00
-1	Res Wt On 2mm Sieve:	0.00	0.00	100.00
GRAVEL WT RETAINED:		0.00		
TOTAL WT < 2mm:		30.32		
SAND				
0	Res Wt On 1mm Sieve:	0.01	SAND % 0.03	0.03 99.97
1	Res Wt On 500um Sieve:	0.01	0.03	0.03 99.93
2	Res Wt On 250um Sieve:	0.06	0.20	0.20 99.74
3	Res Wt On 125um Sieve:	0.09	0.30	0.30 99.44
4	Res Wt On 63um Sieve:	1.09	3.59	3.59 95.84
SAND WT RETAINED:		1.26		
TOTAL WT < 4 PHI:		29.06		

SEDIGRAPH RESULTS				
PHI SIZE:		RETAINED %	% TOTAL WEIGHT	% TOTAL PASSING
5.00	31.25um	2.50	2.40	93.45
6.00	15.63um	8.50	8.15	85.30
7.00	7.81um	15.80	15.14	70.16
8.00	3.91um	16.10	15.43	54.73
9.00	1.95um	10.70	10.26	44.47
10.00	0.98um	5.30	5.08	39.39
11.00	0.49um	4.20	4.03	35.37

TOTAL PERCENTAGES	
% GRAVEL:	0.00
% SAND:	4.16
% SILT	51.37
% CLAY:	44.47
% F CLAY:	35.37

SIZE	% WEIGHT	CUM %
64000	0.00	100.00
32000	0.00	100.00
16000	0.00	100.00
8000	0.00	100.00
4000	0.00	100.00
2000	0.00	100.00
1000	0.03	99.97
500	0.03	99.93
250	0.20	99.74
125	0.30	99.44
63	3.59	95.84
31.25	2.40	93.45
15.63	8.15	85.30
7.81	15.14	70.16
3.91	15.43	54.73
1.95	10.26	44.47
0.98	5.08	39.39
0.49	4.03	35.37
SUM	45.27	



PARTICLE SIZE ANALYSIS

LAB. No: 4551		UNIT: F2U2 a		
LOCATION: Westbury				
SIEVING RESULTS				
SAMPLE Wt: 101.86				
PHI SIZE:		% TOTAL WEIGHT	% TOTAL PASSING	
GRAVEL				
-6	Res Wt On 64mm Sieve:	0.00	0.00	100.00
-5	Res Wt On 32mm Sieve:	0.00	0.00	100.00
-4	Res Wt On 16mm Sieve:	0.00	0.00	100.00
-3	Res Wt On 8mm Sieve:	0.00	0.00	100.00
-2	Res Wt On 4mm Sieve:	0.00	0.00	100.00
-1	Res Wt On 2mm Sieve:	0.00	0.00	100.00
GRAVEL WT RETAINED:		0.00		
TOTAL WT < 2mm:		101.86		
SAND				
0	Res Wt On 1mm Sieve:	0.00	SAND %	
			0.00	100.00
1	Res Wt On 500um Sieve:	0.01	0.01	99.99
2	Res Wt On 250um Sieve:	0.04	0.04	99.95
3	Res Wt On 125um Sieve:	0.80	0.79	99.17
4	Res Wt On 63um Sieve:	54.69	53.69	45.47
SAND WT RETAINED:		55.54		
TOTAL WT < 4 PHI:		46.32		

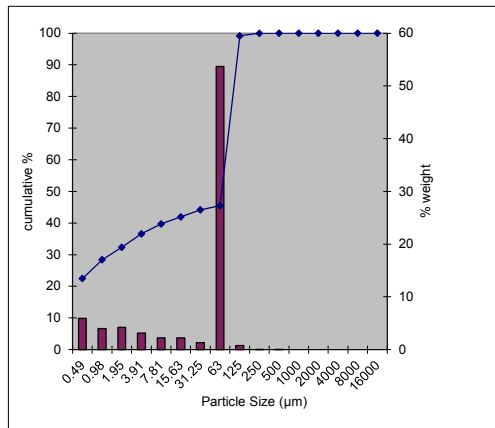
SEDIGRAPH RESULTS

PHI SIZE:		RETAINED %	% TOTAL WEIGHT	% TOTAL PASSING
5.00	31.25um	2.90	1.32	44.16
6.00	15.63um	4.90	2.23	41.93
7.00	7.81um	4.90	2.23	39.70
8.00	3.91um	6.90	3.14	36.56
9.00	1.95um	9.30	4.23	32.33
10.00	0.98um	8.70	3.96	28.38
11.00	0.49um	13.00	5.91	22.46

TOTAL PERCENTAGES

% GRAVEL:	0.00
% SAND:	54.53
% SILT	13.14
% CLAY:	32.33
% F CLAY:	22.46

SIZE	% WEIGHT	CUM %
64000mm	0.00	100.00
32000um	0.00	100.00
16000	0.00	100.00
8000	0.00	100.00
4000	0.00	100.00
2000	0.00	100.00
1000	0.00	100.00
500	0.01	99.99
250	0.04	99.95
125	0.79	99.17
63	53.69	45.47
31.25	1.32	44.16
15.63	2.23	41.93
7.81	2.23	39.70
3.91	3.14	36.56
1.95	4.23	32.33
0.98	3.96	28.38
0.49	5.91	22.46
SUM	63.44	

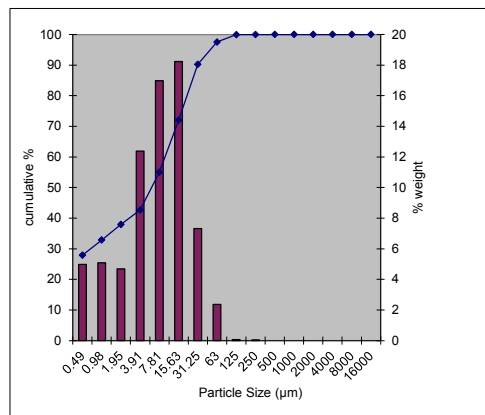


PARTICLE SIZE ANALYSIS				
LAB. No:	4552	UNIT	F2U2 b	
LOCATION:	Westbury			
SIEVING RESULTS				
SAMPLE Wt:	31.63			
PHI SIZE:			% TOTAL WEIGHT	% TOTAL PASSING
GRAVEL				
-6	Res Wt On 64mm Sieve:	0.00	0.00	100.00
-5	Res Wt On 32mm Sieve:	0.00	0.00	100.00
-4	Res Wt On 16mm Sieve:	0.00	0.00	100.00
-3	Res Wt On 8mm Sieve:	0.00	0.00	100.00
-2	Res Wt On 4mm Sieve:	0.00	0.00	100.00
-1	Res Wt On 2mm Sieve:	0.00	0.00	100.00
GRAVEL WT RETAINED:		0.00		
TOTAL WT < 2mm:		31.63		
SAND				
			SAND %	
0	Res Wt On 1mm Sieve:	0.00	0.00	100.00
1	Res Wt On 500um Sieve:	0.00	0.00	100.00
2	Res Wt On 250um Sieve:	0.01	0.03	99.97
3	Res Wt On 125um Sieve:	0.02	0.06	99.91
4	Res Wt On 63um Sieve:	0.75	2.37	97.53
SAND WT RETAINED:		0.78		
TOTAL WT < 4 PHI:		30.85		

SEDIGRAPH RESULTS				
PHI SIZE:		RETAINED %	% TOTAL WEIGHT	% TOTAL PASSING
5.00	31.25um	7.50	7.32	90.22
6.00	15.63um	18.70	18.24	71.98
7.00	7.81um	17.40	16.97	55.01
8.00	3.91um	12.70	12.39	42.62
9.00	1.95um	4.80	4.68	37.94
10.00	0.98um	5.20	5.07	32.87
11.00	0.49um	5.10	4.97	27.89

TOTAL PERCENTAGES	
% GRAVEL:	0.00
% SAND:	2.47
% SILT:	59.59
% CLAY:	37.94
% F CLAY:	27.89

SIZE	% WEIGHT	CUM %
64000mm	0.00	100.00
32000um	0.00	100.00
16000	0.00	100.00
8000	0.00	100.00
4000	0.00	100.00
2000	0.00	100.00
1000	0.00	100.00
500	0.00	100.00
250	0.03	99.97
125	0.06	99.91
63	2.37	97.53
31.25	7.32	90.22
15.63	18.24	71.98
7.81	16.97	55.01
3.91	12.39	42.62
1.95	4.68	37.94
0.98	5.07	32.87
0.49	4.97	27.89
SUM	57.38	

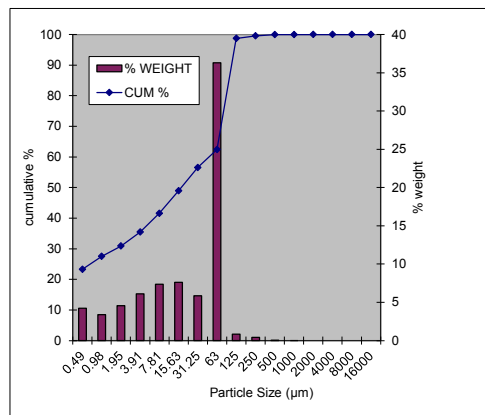


PARTICLE SIZE ANALYSIS				
LAB. No:	4560	UNIT	F2U3	
LOCATION:	Westbury			
SIEVING RESULTS				
SAMPLE Wt:	99.73			
PHI SIZE:			% TOTAL WEIGHT	% TOTAL PASSING
GRAVEL				
-6	Res Wt On 64mm Sieve:	0.00	0.00	100.00
-5	Res Wt On 32mm Sieve:	0.00	0.00	100.00
-4	Res Wt On 16mm Sieve:	0.00	0.00	100.00
-3	Res Wt On 8mm Sieve:	0.00	0.00	100.00
-2	Res Wt On 4mm Sieve:	0.00	0.00	100.00
-1	Res Wt On 2mm Sieve:	0.00	0.00	100.00
GRAVEL WT RETAINED:		0.00		
TOTAL WT < 2mm:		99.73		
SAND				
			SAND %	
0	Res Wt On 1mm Sieve:	0.01	0.01	99.99
1	Res Wt On 500um Sieve:	0.04	0.04	99.95
2	Res Wt On 250um Sieve:	0.40	0.40	99.55
3	Res Wt On 125um Sieve:	0.83	0.83	98.72
4	Res Wt On 63um Sieve:	36.21	36.31	62.41
SAND WT RETAINED:		37.49		
TOTAL WT < 4 PHI:		62.24		

SEDIGRAPH RESULTS				
PHI SIZE:		RETAINED %	% TOTAL WEIGHT	% TOTAL PASSING
5.00	31.25um	9.40	5.87	56.54
6.00	15.63um	12.20	7.61	48.93
7.00	7.81um	11.80	7.36	41.56
8.00	3.91um	9.80	6.12	35.45
9.00	1.95um	7.30	4.56	30.89
10.00	0.98um	5.40	3.37	27.52
11.00	0.49um	6.80	4.24	23.28

TOTAL PERCENTAGES	
% GRAVEL:	0.00
% SAND:	37.59
% SILT	31.52
% CLAY:	30.89
% F CLAY:	23.28

SIZE	% WEIGHT	CUM %
64000mm	0.00	100.00
32000um	0.00	100.00
16000	0.00	100.00
8000	0.00	100.00
4000	0.00	100.00
2000	0.00	100.00
1000	0.01	99.99
500	0.04	99.95
250	0.40	99.55
125	0.83	98.72
63	36.31	62.41
31.25	5.87	56.54
15.63	7.61	48.93
7.81	7.36	41.56
3.91	6.12	35.45
1.95	4.56	30.89
0.98	3.37	27.52
0.49	4.24	23.28
SUM	64.55	

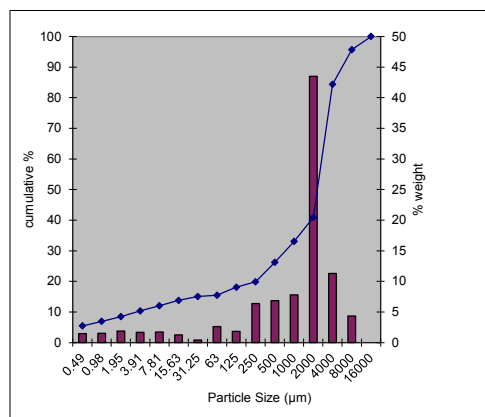


PARTICLE SIZE ANALYSIS				
LAB. No:	4555	UNIT	F3U2_a	
LOCATION:	Westbury			
SIEVING RESULTS				
SAMPLE Wt:	230.00			
PHI SIZE:			% TOTAL WEIGHT	% TOTAL PASSING
GRAVEL				
-6	Res Wt On 64mm Sieve:	0.00	0.00	100.00
-5	Res Wt On 32mm Sieve:	0.00	0.00	100.00
-4	Res Wt On 16mm Sieve:	0.00	0.00	100.00
-3	Res Wt On 8mm Sieve:	10.00	4.35	95.65
-2	Res Wt On 4mm Sieve:	26.00	11.30	84.35
-1	Res Wt On 2mm Sieve:	100.00	43.48	40.87
GRAVEL WT RETAINED:		136.00		
TOTAL WT < 2mm:		101.43		
SAND				
			SAND %	
0	Res Wt On 1mm Sieve:	19.36	19.09	7.80
1	Res Wt On 500um Sieve:	17.02	16.78	6.86
2	Res Wt On 250um Sieve:	15.78	15.56	6.36
3	Res Wt On 125um Sieve:	4.50	4.44	1.81
4	Res Wt On 63um Sieve:	6.44	6.35	2.59
SAND WT RETAINED:		63.10		
TOTAL WT < 4 PHI:		35.52		

SEDIGRAPH RESULTS				
PHI SIZE:		RETAINED %	% TOTAL WEIGHT	% TOTAL PASSING
5.00	31.25um	2.70	0.42	15.03
6.00	15.63um	8.20	1.27	13.76
7.00	7.81um	11.20	1.73	12.03
8.00	3.91um	11.00	1.70	10.33
9.00	1.95um	12.10	1.87	8.46
10.00	0.98um	9.90	1.53	6.93
11.00	0.49um	9.60	1.48	5.45

TOTAL PERCENTAGES	
% GRAVEL:	59.13
% SAND:	25.43
% SILT	6.98
% CLAY:	8.46
% F CLAY:	5.45

SIZE	% WEIGHT	CUM %
64000mm	0.00	100.00
32000um	0.00	100.00
16000	0.00	100.00
8000	4.35	95.65
4000	11.30	84.35
2000	43.48	40.87
1000	7.80	33.07
500	6.86	26.21
250	6.36	19.85
125	1.81	18.04
63	2.59	15.44
31.25	0.42	15.03
15.63	1.27	13.76
7.81	1.73	12.03
3.91	1.70	10.33
1.95	1.87	8.46
0.98	1.53	6.93
0.49	1.48	5.45
SUM	89.67	

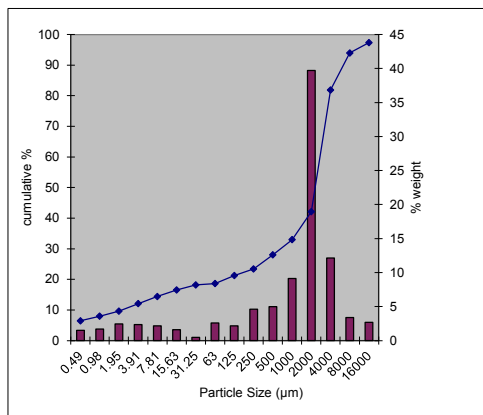


PARTICLE SIZE ANALYSIS				
LAB. No:	4556	UNIT	F3U2 b	
LOCATION:	Westbury			
SIEVING RESULTS				
SAMPLE Wt:	297.00			
PHI SIZE:			% TOTAL WEIGHT	% TOTAL PASSING
GRAVEL				
-6	Res Wt On 64mm Sieve:	0.00	0.00	100.00
-5	Res Wt On 32mm Sieve:	0.00	0.00	100.00
-4	Res Wt On 16mm Sieve:	8.00	2.69	97.31
-3	Res Wt On 8mm Sieve:	10.00	3.37	93.94
-2	Res Wt On 4mm Sieve:	36.00	12.12	81.82
-1	Res Wt On 2mm Sieve:	118.00	39.73	42.09
GRAVEL WT RETAINED:		172.00		
TOTAL WT < 2mm:		109.22		
SAND				
			SAND %	
0	Res Wt On 1mm Sieve:	23.66	21.66	9.12
1	Res Wt On 500um Sieve:	12.93	11.84	4.98
2	Res Wt On 250um Sieve:	11.94	10.93	4.60
3	Res Wt On 125um Sieve:	5.61	5.14	2.16
4	Res Wt On 63um Sieve:	6.71	6.14	2.59
SAND WT RETAINED:		60.85		
TOTAL WT < 4 PHI:		55.36		

SEDIGRAPH RESULTS				
PHI SIZE:		RETAINED %	% TOTAL WEIGHT	% TOTAL PASSING
5.00	31.25um	2.60	0.48	18.15
6.00	15.63um	8.70	1.62	16.53
7.00	7.81um	11.50	2.14	14.39
8.00	3.91um	12.60	2.35	12.04
9.00	1.95um	13.00	2.42	9.62
10.00	0.98um	9.00	1.68	7.94
11.00	0.49um	8.00	1.49	6.45

TOTAL PERCENTAGES	
% GRAVEL:	57.91
% SAND:	23.45
% SILT	9.02
% CLAY:	9.62
% F CLAY:	6.45

SIZE	% WEIGHT	CUM %
64000mm	0.00	100.00
32000um	0.00	100.00
16000	2.69	97.31
8000	3.37	93.94
4000	12.12	81.82
2000	39.73	42.09
1000	9.12	32.97
500	4.98	27.99
250	4.60	23.39
125	2.16	21.22
63	2.59	18.64
31.25	0.48	18.15
15.63	1.62	16.53
7.81	2.14	14.39
3.91	2.35	12.04
1.95	2.42	9.62
0.98	1.68	7.94
0.49	1.49	6.45
SUM	87.96	

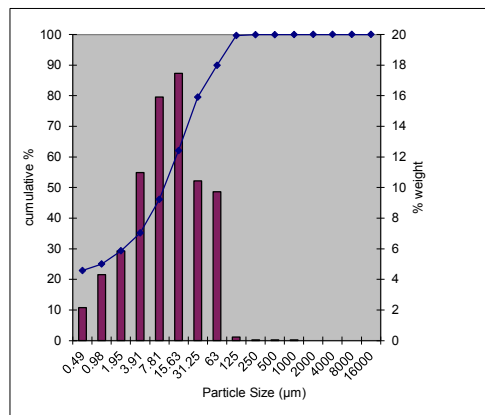


PARTICLE SIZE ANALYSIS				
LAB. No:	4553	UNIT	F3U3_a	
LOCATION:	Westbury			
SIEVING RESULTS				
SAMPLE Wt:	31.45			
PHI SIZE:			% TOTAL WEIGHT	% TOTAL PASSING
GRAVEL				
-6	Res Wt On 64mm Sieve:	0.00	0.00	100.00
-5	Res Wt On 32mm Sieve:	0.00	0.00	100.00
-4	Res Wt On 16mm Sieve:	0.00	0.00	100.00
-3	Res Wt On 8mm Sieve:	0.00	0.00	100.00
-2	Res Wt On 4mm Sieve:	0.00	0.00	100.00
-1	Res Wt On 2mm Sieve:	0.00	0.00	100.00
GRAVEL WT RETAINED:		0.00		
TOTAL WT < 2mm:		31.45		
SAND				
			SAND %	
0	Res Wt On 1mm Sieve:	0.01	0.03	99.97
1	Res Wt On 500um Sieve:	0.01	0.03	99.94
2	Res Wt On 250um Sieve:	0.01	0.03	99.90
3	Res Wt On 125um Sieve:	0.07	0.22	99.68
4	Res Wt On 63um Sieve:	3.06	9.73	89.95
SAND WT RETAINED:		3.16		
TOTAL WT < 4 PHI:		28.29		

SEDIGRAPH RESULTS				
PHI SIZE:		RETAINED %	% TOTAL WEIGHT	% TOTAL PASSING
5.00	31.25um	11.60	10.43	79.52
6.00	15.63um	19.40	17.45	62.07
7.00	7.81um	17.70	15.92	46.15
8.00	3.91um	12.20	10.97	35.17
9.00	1.95um	6.50	5.85	29.32
10.00	0.98um	4.80	4.32	25.01
11.00	0.49um	2.40	2.16	22.85

TOTAL PERCENTAGES	
% GRAVEL:	0.00
% SAND:	10.05
% SILT	60.63
% CLAY:	29.32
% F CLAY:	22.85

SIZE	% WEIGHT	CUM %
64000mm	0.00	100.00
32000um	0.00	100.00
16000	0.00	100.00
8000	0.00	100.00
4000	0.00	100.00
2000	0.00	100.00
1000	0.03	99.97
500	0.03	99.94
250	0.03	99.90
125	0.22	99.68
63	9.73	89.95
31.25	10.43	79.52
15.63	17.45	62.07
7.81	15.92	46.15
3.91	10.97	35.17
1.95	5.85	29.32
0.98	4.32	25.01
0.49	2.16	22.85
SUM	64.83	

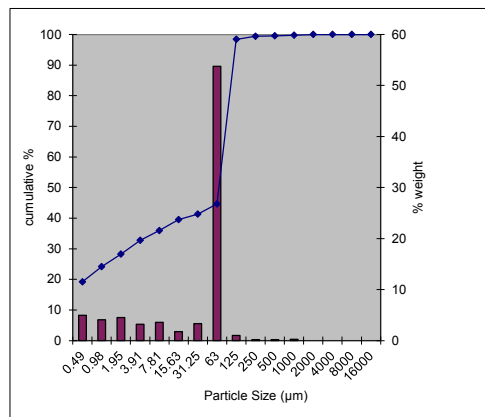


PARTICLE SIZE ANALYSIS				
LAB. No:	4554	UNIT	F3U3_b	
LOCATION:	Westbury			
SIEVING RESULTS				
SAMPLE Wt:	105.62			
PHI SIZE:			% TOTAL WEIGHT	% TOTAL PASSING
GRAVEL				
-6	Res Wt On 64mm Sieve:	0.00	0.00	100.00
-5	Res Wt On 32mm Sieve:	0.00	0.00	100.00
-4	Res Wt On 16mm Sieve:	0.00	0.00	100.00
-3	Res Wt On 8mm Sieve:	0.00	0.00	100.00
-2	Res Wt On 4mm Sieve:	0.00	0.00	100.00
-1	Res Wt On 2mm Sieve:	0.00	0.00	100.00
GRAVEL WT RETAINED:		0.00		
TOTAL WT < 2mm:		105.62		
SAND				
			SAND %	
0	Res Wt On 1mm Sieve:	0.26	0.25	99.75
1	Res Wt On 500um Sieve:	0.20	0.19	99.56
2	Res Wt On 250um Sieve:	0.17	0.16	99.40
3	Res Wt On 125um Sieve:	1.05	0.99	98.41
4	Res Wt On 63um Sieve:	56.78	53.76	44.65
SAND WT RETAINED:		58.46		
TOTAL WT < 4 PHI:		47.16		

SEDIGRAPH RESULTS				
PHI SIZE:		RETAINED %	% TOTAL WEIGHT	% TOTAL PASSING
5.00	31.25um	7.50	3.35	41.30
6.00	15.63um	4.00	1.79	39.52
7.00	7.81um	8.00	3.57	35.94
8.00	3.91um	7.10	3.17	32.77
9.00	1.95um	10.10	4.51	28.26
10.00	0.98um	9.20	4.11	24.16
11.00	0.49um	11.10	4.96	19.20

TOTAL PERCENTAGES	
% GRAVEL:	0.00
% SAND:	55.35
% SILT:	16.39
% CLAY:	28.26
% F CLAY:	19.20

SIZE	% WEIGHT	CUM %
64000mm	0.00	100.00
32000um	0.00	100.00
16000	0.00	100.00
8000	0.00	100.00
4000	0.00	100.00
2000	0.00	100.00
1000	0.25	99.75
500	0.19	99.56
250	0.16	99.40
125	0.99	98.41
63	53.76	44.65
31.25	3.35	41.30
15.63	1.79	39.52
7.81	3.57	35.94
3.91	3.17	32.77
1.95	4.51	28.26
0.98	4.11	24.16
0.49	4.96	19.20
SUM	67.23	

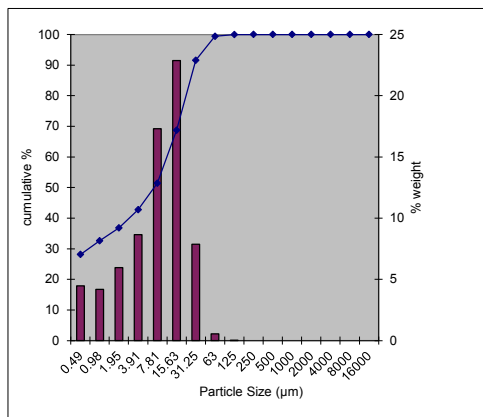


PARTICLE SIZE ANALYSIS				
LAB. No:	4557	UNIT	F4U3	
LOCATION:	Westbury			
SIEVING RESULTS				
SAMPLE Wt:	31.68			
PHI SIZE:			% TOTAL WEIGHT	% TOTAL PASSING
GRAVEL				
-6	Res Wt On 64mm Sieve:	0.00	0.00	100.00
-5	Res Wt On 32mm Sieve:	0.00	0.00	100.00
-4	Res Wt On 16mm Sieve:	0.00	0.00	100.00
-3	Res Wt On 8mm Sieve:	0.00	0.00	100.00
-2	Res Wt On 4mm Sieve:	0.00	0.00	100.00
-1	Res Wt On 2mm Sieve:	0.00	0.00	100.00
GRAVEL WT RETAINED:		0.00		
TOTAL WT < 2mm:		31.68		
SAND				
			SAND %	
0	Res Wt On 1mm Sieve:	0.00	0.00	100.00
1	Res Wt On 500um Sieve:	0.00	0.00	100.00
2	Res Wt On 250um Sieve:	0.00	0.00	100.00
3	Res Wt On 125um Sieve:	0.01	0.03	99.97
4	Res Wt On 63um Sieve:	0.17	0.54	99.43
SAND WT RETAINED:		0.18		
TOTAL WT < 4 PHI:		31.50		

SEDIGRAPH RESULTS				
PHI SIZE:		RETAINED %	% TOTAL WEIGHT	% TOTAL PASSING
5.00	31.25um	7.90	7.86	91.58
6.00	15.63um	23.00	22.87	68.71
7.00	7.81um	17.40	17.30	51.41
8.00	3.91um	8.70	8.65	42.76
9.00	1.95um	6.00	5.97	36.79
10.00	0.98um	4.20	4.18	32.61
11.00	0.49um	4.50	4.47	28.14

TOTAL PERCENTAGES	
% GRAVEL:	0.00
% SAND:	0.57
% SILT	62.64
% CLAY:	36.79
% F CLAY:	28.14

SIZE	% WEIGHT	CUM %
64000mm	0.00	100.00
32000um	0.00	100.00
16000	0.00	100.00
8000	0.00	100.00
4000	0.00	100.00
2000	0.00	100.00
1000	0.00	100.00
500	0.00	100.00
250	0.00	100.00
125	0.03	99.97
63	0.54	99.43
31.25	7.86	91.58
15.63	22.87	68.71
7.81	17.30	51.41
3.91	8.65	42.76
1.95	5.97	36.79
0.98	4.18	32.61
0.49	4.47	28.14
SUM	57.24	

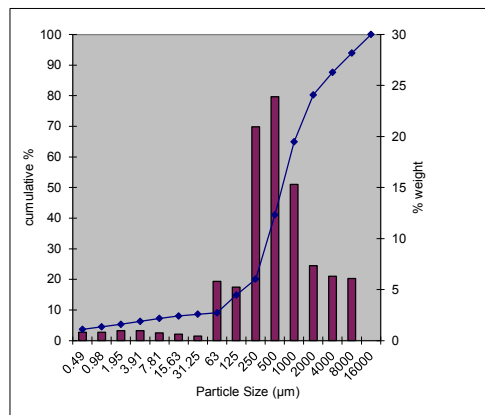


PARTICLE SIZE ANALYSIS				
LAB. No:	4558	UNIT	FSU3	
LOCATION:	Westbury			
SIEVING RESULTS				
SAMPLE Wt:	476.00			
PHI SIZE:			% TOTAL WEIGHT	% TOTAL PASSING
GRAVEL				
-6	Res Wt On 64mm Sieve:	0.00	0.00	100.00
-5	Res Wt On 32mm Sieve:	0.00	0.00	100.00
-4	Res Wt On 16mm Sieve:	0.00	0.00	100.00
-3	Res Wt On 8mm Sieve:	29.00	6.09	93.91
-2	Res Wt On 4mm Sieve:	30.00	6.30	87.61
-1	Res Wt On 2mm Sieve:	35.00	7.35	80.25
GRAVEL WT RETAINED:		94.00		
TOTAL WT < 2mm:		101.52		
SAND				
			SAND %	
0	Res Wt On 1mm Sieve:	19.38	19.09	15.32
1	Res Wt On 500um Sieve:	30.22	29.77	23.89
2	Res Wt On 250um Sieve:	26.51	26.11	20.96
3	Res Wt On 125um Sieve:	6.61	6.51	5.23
4	Res Wt On 63um Sieve:	7.34	7.23	5.80
SAND WT RETAINED:		90.06		
TOTAL WT < 4 PHI:		43.12		

SEDIGRAPH RESULTS				
PHI SIZE:		RETAINED %	% TOTAL WEIGHT	% TOTAL PASSING
5.00	31.25um	4.90	0.44	8.62
6.00	15.63um	6.80	0.62	8.00
7.00	7.81um	8.40	0.76	7.24
8.00	3.91um	10.60	0.96	6.28
9.00	1.95um	10.80	0.98	5.30
10.00	0.98um	8.90	0.81	4.49
11.00	0.49um	9.10	0.82	3.67

TOTAL PERCENTAGES	
% GRAVEL:	19.75
% SAND:	71.19
% SILT:	3.76
% CLAY:	5.30
% F CLAY:	3.67

SIZE	% WEIGHT	CUM %
64000mm	0.00	100.00
32000um	0.00	100.00
16000	0.00	100.00
8000	6.09	93.91
4000	6.30	87.61
2000	7.35	80.25
1000	15.32	64.93
500	23.89	41.04
250	20.96	20.09
125	5.23	14.86
63	5.80	9.06
31.25	0.44	8.62
15.63	0.62	8.00
7.81	0.76	7.24
3.91	0.96	6.28
1.95	0.98	5.30
0.98	0.81	4.49
0.49	0.82	3.67
SUM	93.72	

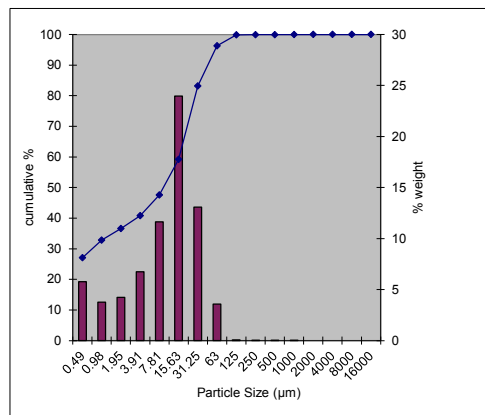


PARTICLE SIZE ANALYSIS				
LAB. No:	4559	UNIT	F6U4	
LOCATION:	Westbury			
SIEVING RESULTS				
SAMPLE Wt:	32.61			
PHI SIZE:			% TOTAL WEIGHT	% TOTAL PASSING
GRAVEL				
-6	Res Wt On 64mm Sieve:	0.00	0.00	100.00
-5	Res Wt On 32mm Sieve:	0.00	0.00	100.00
-4	Res Wt On 16mm Sieve:	0.00	0.00	100.00
-3	Res Wt On 8mm Sieve:	0.00	0.00	100.00
-2	Res Wt On 4mm Sieve:	0.00	0.00	100.00
-1	Res Wt On 2mm Sieve:	0.00	0.00	100.00
GRAVEL WT RETAINED:		0.00		
TOTAL WT < 2mm:		32.61		
SAND				
			SAND %	
0	Res Wt On 1mm Sieve:	0.01	0.03	99.97
1	Res Wt On 500um Sieve:	0.01	0.03	99.94
2	Res Wt On 250um Sieve:	0.01	0.03	99.91
3	Res Wt On 125um Sieve:	0.02	0.06	99.85
4	Res Wt On 63um Sieve:	1.17	3.59	96.26
SAND WT RETAINED:		1.22		
TOTAL WT < 4 PHI:		31.39		

SEDIGRAPH RESULTS				
PHI SIZE:		RETAINED %	% TOTAL WEIGHT	% TOTAL PASSING
5.00	31.25um	13.60	13.09	83.17
6.00	15.63um	24.90	23.97	59.20
7.00	7.81um	12.10	11.65	47.55
8.00	3.91um	7.00	6.74	40.81
9.00	1.95um	4.40	4.24	36.58
10.00	0.98um	3.90	3.75	32.82
11.00	0.49um	6.00	5.78	27.05

TOTAL PERCENTAGES	
% GRAVEL:	0.00
% SAND:	3.74
% SILT	59.68
% CLAY:	36.58
% F CLAY:	27.05

SIZE	% WEIGHT	CUM %
64000mm	0.00	100.00
32000um	0.00	100.00
16000	0.00	100.00
8000	0.00	100.00
4000	0.00	100.00
2000	0.00	100.00
1000	0.03	99.97
500	0.03	99.94
250	0.03	99.91
125	0.06	99.85
63	3.59	96.26
31.25	13.09	83.17
15.63	23.97	59.20
7.81	11.65	47.55
3.91	6.74	40.81
1.95	4.24	36.58
0.98	3.75	32.82
0.49	5.78	27.05
SUM	59.19	



SAMPLE STATISTICS

SAMPLE IDENTITY: **4549** UNIT **F1U1**
 SAMPLE TYPE: Bimodal, Poorly Sorted
 SEDIMENT NAME: Medium Silt

ANALYST & DATE: Adams, 16/01/2015
 TEXTURAL GROUP: Mud

	μm		ϕ		GRAIN SIZE DISTRIBUTION		
MODE 1:	11.72	6.500			GRAVEL: 0.0%		COARSE SAND: 0.4%
MODE 2:	0.735	10.49			SAND: 3.5%		MEDIUM SAND: 0.3%
MODE 3:					MUD: 96.5%		FINE SAND: 0.3%
D ₁₀ :	0.932	5.075					V FINE SAND: 1.3%
MEDIAN or D ₅₀ :	9.202	6.764			V COARSE GRAVEL: 0.0%		V COARSE SILT: 4.9%
D ₉₀ :	29.67	10.07			COARSE GRAVEL: 0.0%		COARSE SILT: 20.9%
(D ₉₀ / D ₁₀):	31.84	1.984			MEDIUM GRAVEL: 0.0%		MEDIUM SILT: 27.0%
(D ₉₀ - D ₁₀):	28.74	4.993			FINE GRAVEL: 0.0%		FINE SILT: 14.3%
(D ₇₅ / D ₂₅):	6.019	1.447			V FINE GRAVEL: 0.0%		V FINE SILT: 11.2%
(D ₇₅ - D ₂₅):	15.06	2.590			V COARSE SAND: 1.2%		CLAY: 18.1%
	METHOD OF MOMENTS			FOLK & WARD METHOD			
	Arithmetic	Geometric	Logarithmic	Geometric	Logarithmic	Description	
	μm	μm	ϕ	μm	ϕ		
MEAN (\bar{x}):	35.63	7.629	7.034	7.113	7.135	Fine Silt	
SORTING (σ):	169.4	4.043	2.015	3.793	1.923	Poorly Sorted	
SKEWNESS (Sk):	7.990	0.403	-0.403	-0.247	0.247	Fine Skewed	
KURTOSIS (K):	67.49	4.487	4.487	0.986	0.986	Mesokurtic	

SAMPLE STATISTICS

SAMPLE IDENTITY: **4547** UNIT **F1U2a**
 SAMPLE TYPE: Trimodal, Very Poorly Sorted
 SEDIMENT NAME: Very Fine Silty Sandy Medium Gravel

ANALYST & DATE: Adams, 16/01/2015
 TEXTURAL GROUP: Muddy Sandy Gravel

	μm		ϕ		GRAIN SIZE DISTRIBUTION		
	μm	ϕ					
MODE 1:	12000.0	-3.500			GRAVEL: 62.7%		COARSE SAND: 11.3%
MODE 2:	3000.0	-1.500			SAND: 26.9%		MEDIUM SAND: 5.7%
MODE 3:	750.0	0.500			MUD: 10.4%		FINE SAND: 1.5%
D ₁₀ :	33.25	-3.689					V FINE SAND: 1.8%
MEDIAN or D ₅₀ :	3061.3	-1.614			V COARSE GRAVEL: 0.0%		V COARSE SILT: 0.4%
D ₉₀ :	12896.3	4.911			COARSE GRAVEL: 0.0%		COARSE SILT: 1.1%
(D ₉₀ / D ₁₀):	387.9	-1.331			MEDIUM GRAVEL: 32.1%		MEDIUM SILT: 1.7%
(D ₉₀ - D ₁₀):	12863.1	8.600			FINE GRAVEL: 9.9%		FINE SILT: 2.0%
(D ₇₅ / D ₂₅):	13.27	-0.158			V FINE GRAVEL: 20.7%		V FINE SILT: 2.1%
(D ₇₅ - D ₂₅):	8629.2	3.731			V COARSE SAND: 6.5%		CLAY: 3.1%
	METHOD OF MOMENTS			FOLK & WARD METHOD			
	Arithmetic	Geometric	Logarithmic	Geometric	Logarithmic	Description	
	μm	μm	ϕ	μm	ϕ		
MEAN (\bar{x}):	5279.9	1562.5	-0.644	2250.1	-1.170	Very Fine Gravel	
SORTING (σ):	4903.2	11.00	3.460	8.510	3.089	Very Poorly Sorted	
SKEWNESS (Sk):	0.463	-1.638	1.638	-0.444	0.444	Very Fine Skewed	
KURTOSIS (K):	1.486	5.084	5.084	1.314	1.314	Leptokurtic	

SAMPLE STATISTICS

SAMPLE IDENTITY: **4548** UNIT **F1U2_b**
 SAMPLE TYPE: Trimodal, Very Poorly Sorted
 SEDIMENT NAME: Fine Silty Sandy Very Fine Gravel

ANALYST & DATE: Adams, 16/01/2015
 TEXTURAL GROUP: Muddy Sandy Gravel

	μm		ϕ		GRAIN SIZE DISTRIBUTION			
MODE 1:	3000.0		-1.500		GRAVEL: 57.5%		COARSE SAND: 10.2%	
MODE 2:	12000.0		-3.500		SAND: 31.2%		MEDIUM SAND: 6.6%	
MODE 3:	750.0		0.500		MUD: 11.3%		FINE SAND: 2.5%	
D ₁₀ :	21.64		-3.193				V FINE SAND: 3.1%	
MEDIAN or D ₅₀ :	2331.2		-1.221		V COARSE GRAVEL: 0.0%		V COARSE SILT: 0.5%	
D ₉₀ :	9146.8		5.530		COARSE GRAVEL: 0.0%		COARSE SILT: 1.5%	
(D ₉₀ / D ₁₀):	422.6		-1.732		MEDIUM GRAVEL: 12.4%		MEDIUM SILT: 2.1%	
(D ₉₀ - D ₁₀):	9125.2		8.723		FINE GRAVEL: 11.3%		FINE SILT: 2.1%	
(D ₇₅ / D ₂₅):	7.019		-0.434		V FINE GRAVEL: 33.8%		V FINE SILT: 2.0%	
(D ₇₅ - D ₂₅):	3337.5		2.811		V COARSE SAND: 8.9%		CLAY: 3.0%	
	METHOD OF MOMENTS			FOLK & WARD METHOD				
	Arithmetic	Geometric	Logarithmic	Geometric	Logarithmic	Description		
	μm	μm	ϕ	μm	ϕ			
MEAN (\bar{x}):	3420.5	1049.1	-0.069	1428.8	-0.515	Very Coarse Sand		
SORTING (σ):	3676.5	9.819	3.296	8.101	3.018	Very Poorly Sorted		
SKEWNESS (Sk):	1.394	-1.586	1.586	-0.506	0.506	Very Fine Skewed		
KURTOSIS (K):	3.889	4.932	4.932	1.692	1.692	Very Leptokurtic		

SAMPLE STATISTICS

SAMPLE IDENTITY: **4550** UNIT **F1U3**
 SAMPLE TYPE: Bimodal, Poorly Sorted
 SEDIMENT NAME: Fine Silt

ANALYST & DATE: Adams, 16/01/2015
 TEXTURAL GROUP: Mud

	μm		ϕ		GRAIN SIZE DISTRIBUTION			
MODE 1:	5.860	7.500			GRAVEL: 0.0%		COARSE SAND: 0.0%	
MODE 2:	94.00	3.494			SAND: 6.5%		MEDIUM SAND: 0.3%	
MODE 3:					MUD: 93.5%		FINE SAND: 0.5%	
D ₁₀ :	1.363	4.964					V FINE SAND: 5.6%	
MEDIAN or D ₅₀ :	6.988	7.161			V COARSE GRAVEL: 0.0%		V COARSE SILT: 3.7%	
D ₉₀ :	32.05	9.519			COARSE GRAVEL: 0.0%		COARSE SILT: 12.6%	
(D ₉₀ / D ₁₀):	23.52	1.918			MEDIUM GRAVEL: 0.0%		MEDIUM SILT: 23.4%	
(D ₉₀ - D ₁₀):	30.68	4.556			FINE GRAVEL: 0.0%		FINE SILT: 23.9%	
(D ₇₅ / D ₂₅):	4.648	1.364			V FINE GRAVEL: 0.0%		V FINE SILT: 15.8%	
(D ₇₅ - D ₂₅):	11.47	2.217			V COARSE SAND: 0.0%		CLAY: 14.1%	
	METHOD OF MOMENTS			FOLK & WARD METHOD				
	Arithmetic	Geometric	Logarithmic	Geometric	Logarithmic	Description		
	μm	μm	ϕ	μm	ϕ			
MEAN (\bar{x}):	17.77	7.123	7.133	6.948	7.169	Fine Silt		
SORTING (σ):	47.67	3.417	1.773	3.562	1.833	Poorly Sorted		
SKEWNESS (Sk):	17.37	0.269	-0.269	0.027	-0.027	Symmetrical		
KURTOSIS (K):	470.6	3.158	3.158	1.194	1.194	Leptokurtic		

SAMPLE STATISTICS

SAMPLE IDENTITY: 4551 UNIT F2U2_a
 SAMPLE TYPE: Unimodal, Very Poorly Sorted
 SEDIMENT NAME: Muddy Very Fine Sand

ANALYST & DATE: Adams, 16/01/2015
 TEXTURAL GROUP: Muddy Sand

	μm	ϕ	GRAIN SIZE DISTRIBUTION			
			GRAVEL: 0.0%	SAND: 70.3%	MUD: 29.7%	
MODE 1:	94.00	3.494				
MODE 2:						
MODE 3:						
D ₁₀ :	1.350	3.127				
MEDIAN or D ₅₀ :	77.03	3.698	V COARSE GRAVEL: 0.0%			V FINE SAND: 69.3%
D ₉₀ :	114.4	9.532	COARSE GRAVEL: 0.0%			COARSE SILT: 2.9%
(D ₉₀ / D ₁₀):	84.75	3.048	MEDIUM GRAVEL: 0.0%			MEDIUM SILT: 2.9%
(D ₉₀ - D ₁₀):	113.1	6.405	FINE GRAVEL: 0.0%			FINE SILT: 4.1%
(D ₇₅ / D ₂₅):	6.476	1.807	V FINE GRAVEL: 0.0%			V FINE SILT: 5.4%
(D ₇₅ - D ₂₅):	83.42	2.695	V COARSE SAND: 0.0%			CLAY: 12.7%
	METHOD OF MOMENTS			FOLK & WARD METHOD		
	Arithmetic	Geometric	Logarithmic	Geometric	Logarithmic	Description
	μm	μm	ϕ	μm	ϕ	
MEAN (\bar{x}):	69.62	33.05	4.919	29.08	5.104	Coarse Silt
SORTING (σ):	42.82	5.437	2.443	5.279	2.400	Very Poorly Sorted
SKEWNESS (Sk):	0.072	-1.321	1.321	-0.818	0.818	Very Fine Skewed
KURTOSIS (K):	11.71	3.100	3.100	1.107	1.107	Mesokurtic

SAMPLE STATISTICS

SAMPLE IDENTITY: **4552** UNIT **F2U2_b**
 SAMPLE TYPE: Bimodal, Poorly Sorted
 SEDIMENT NAME: Coarse Silt

ANALYST & DATE: Adams, 16/01/2015
 TEXTURAL GROUP: Mud

	μm	ϕ	GRAIN SIZE DISTRIBUTION				
			GRAVEL: 0.0%	SAND: 3.5%	MUD: 96.5%		
MODE 1:	23.44	5.500				COARSE SAND: 0.0%	
MODE 2:	1.465	9.499				MEDIUM SAND: 0.0%	
MODE 3:						FINE SAND: 0.1%	
D ₁₀ :	1.328	4.645				V FINE SAND: 3.4%	
MEDIAN or D ₅₀ :	11.26	6.473	V COARSE GRAVEL: 0.0%			V COARSE SILT: 10.0%	
D ₉₀ :	39.97	9.556	COARSE GRAVEL: 0.0%			COARSE SILT: 25.3%	
(D ₉₀ / D ₁₀):	30.10	2.057	MEDIUM GRAVEL: 0.0%			MEDIUM SILT: 23.5%	
(D ₉₀ - D ₁₀):	38.64	4.912	FINE GRAVEL: 0.0%			FINE SILT: 17.2%	
(D ₇₅ / D ₂₅):	4.859	1.418	V FINE GRAVEL: 0.0%			V FINE SILT: 6.5%	
(D ₇₅ - D ₂₅):	18.15	2.281	V COARSE SAND: 0.0%			CLAY: 13.9%	
			METHOD OF MOMENTS		FOLK & WARD METHOD		
	Arithmetic	Geometric	Logarithmic	Geometric	Logarithmic	Description	
	μm	μm	ϕ	μm	ϕ		
MEAN (\bar{x}):	18.23	9.440	6.727	9.289	6.750	Medium Silt	
SORTING (σ):	21.20	3.385	1.759	3.541	1.824	Poorly Sorted	
SKEWNESS (Sk):	4.029	-0.513	0.513	-0.236	0.236	Fine Skewed	
KURTOSIS (K):	42.56	2.716	2.716	1.100	1.100	Mesokurtic	

SAMPLE STATISTICS

SAMPLE IDENTITY: **4560** UNIT **F2U3**
 SAMPLE TYPE: Bimodal, Very Poorly Sorted
 SEDIMENT NAME: Very Fine Sandy Coarse Silt

ANALYST & DATE: Adams, 16/01/2015
 TEXTURAL GROUP: Sandy Mud

	μm		ϕ		GRAIN SIZE DISTRIBUTION		
MODE 1:	94.00		3.494		GRAVEL: 0.0%		COARSE SAND: 0.1%
MODE 2:	23.44		5.500		SAND: 49.1%		MEDIUM SAND: 0.5%
MODE 3:					MUD: 50.9%		FINE SAND: 1.1%
D ₁₀ :	1.969		3.174				V FINE SAND: 47.4%
MEDIAN or D ₅₀ :	57.46		4.121		V COARSE GRAVEL: 0.0%		V COARSE SILT: 7.6%
D ₉₀ :	110.8		8.989		COARSE GRAVEL: 0.0%		COARSE SILT: 9.9%
(D ₉₀ / D ₁₀):	56.28		2.832		MEDIUM GRAVEL: 0.0%		MEDIUM SILT: 9.6%
(D ₉₀ - D ₁₀):	108.8		5.815		FINE GRAVEL: 0.0%		FINE SILT: 8.0%
(D ₇₅ / D ₂₅):	10.50		1.973		V FINE GRAVEL: 0.0%		V FINE SILT: 5.9%
(D ₇₅ - D ₂₅):	80.68		3.392		V COARSE SAND: 0.0%		CLAY: 9.9%
	METHOD OF MOMENTS			FOLK & WARD METHOD			
	Arithmetic	Geometric	Logarithmic	Geometric	Logarithmic	Description	
	μm	μm	ϕ	μm	ϕ		
MEAN (\bar{x}):	56.86	25.34	5.303	28.48	5.134	Coarse Silt	
SORTING (σ):	53.76	4.837	2.274	4.705	2.234	Very Poorly Sorted	
SKEWNESS (Sk):	4.711	-0.892	0.892	-0.675	0.675	Very Fine Skewed	
KURTOSIS (K):	89.29	2.592	2.592	0.848	0.848	Platykurtic	

SAMPLE STATISTICS

SAMPLE IDENTITY: **4555** UNIT **F3U2_a**
 SAMPLE TYPE: Unimodal, Very Poorly Sorted
 SEDIMENT NAME: Very Fine Silty Sandy Very Fine Gravel

ANALYST & DATE: Adams, 16/01/2015
 TEXTURAL GROUP: Muddy Sandy Gravel

	μm		ϕ		GRAIN SIZE DISTRIBUTION			
MODE 1:	3000.0		-1.500		GRAVEL: 62.5%		COARSE SAND: 7.3%	
MODE 2:					SAND: 26.9%		MEDIUM SAND: 6.7%	
MODE 3:					MUD: 10.6%		FINE SAND: 1.9%	
D ₁₀ :	29.19		-2.548				V FINE SAND: 2.7%	
MEDIAN or D ₅₀ :	2416.1		-1.273		V COARSE GRAVEL: 0.0%		V COARSE SILT: 0.4%	
D ₉₀ :	5849.2		5.098		COARSE GRAVEL: 0.0%		COARSE SILT: 1.3%	
(D ₉₀ / D ₁₀):	200.4		-2.001		MEDIUM GRAVEL: 4.6%		MEDIUM SILT: 1.8%	
(D ₉₀ - D ₁₀):	5820.0		7.647		FINE GRAVEL: 12.0%		FINE SILT: 1.8%	
(D ₇₅ / D ₂₅):	5.266		-0.320		V FINE GRAVEL: 46.0%		V FINE SILT: 2.0%	
(D ₇₅ - D ₂₅):	2853.0		2.397		V COARSE SAND: 8.2%		CLAY: 3.2%	
		METHOD OF MOMENTS			FOLK & WARD METHOD			
	Arithmetic	Geometric	Logarithmic		Geometric	Logarithmic	Description	
	μm	μm	ϕ		μm	ϕ		
MEAN (\bar{x}):	2859.2	1054.4	-0.076		1392.6	-0.478	Very Coarse Sand	
SORTING (σ):	2669.8	8.832	3.143		6.306	2.657	Very Poorly Sorted	
SKEWNESS (Sk):	1.762	-1.866	1.866		-0.650	0.650	Very Fine Skewed	
KURTOSIS (K):	6.823	5.791	5.791		1.889	1.889	Very Leptokurtic	

SAMPLE STATISTICS

SAMPLE IDENTITY: **4556** UNIT **F3U2_b**
 SAMPLE TYPE: Unimodal, Very Poorly Sorted
 SEDIMENT NAME: Very Fine Silty Sandy Very Fine Gravel

ANALYST & DATE: Adams, 16/01/2015
 TEXTURAL GROUP: Muddy Sandy Gravel

	μm	ϕ	GRAIN SIZE DISTRIBUTION			
			GRAVEL:	SAND:	MUD:	
MODE 1:	3000.0	-1.500	61.9%			COARSE SAND: 5.3%
MODE 2:			25.1%			MEDIUM SAND: 4.9%
MODE 3:			13.0%			FINE SAND: 2.3%
D ₁₀ :	12.35	-2.728				V FINE SAND: 2.8%
MEDIAN or D ₅₀ :	2429.1	-1.280	V COARSE GRAVEL: 0.0%			V COARSE SILT: 0.5%
D ₉₀ :	6626.4	6.339	COARSE GRAVEL: 2.9%			COARSE SILT: 1.7%
(D ₉₀ / D ₁₀):	536.5	-2.324	MEDIUM GRAVEL: 3.6%			MEDIUM SILT: 2.3%
(D ₉₀ - D ₁₀):	6614.0	9.067	FINE GRAVEL: 13.0%			FINE SILT: 2.5%
(D ₇₅ / D ₂₅):	5.643	-0.336	V FINE GRAVEL: 42.5%			V FINE SILT: 2.6%
(D ₇₅ - D ₂₅):	3005.5	2.497	V COARSE SAND: 9.7%			CLAY: 3.4%
			METHOD OF MOMENTS		FOLK & WARD METHOD	
	Arithmetic	Geometric	Logarithmic	Geometric	Logarithmic	Description
	μm	μm	ϕ	μm	ϕ	
MEAN (\bar{x}):	3386.9	998.1	0.003	1158.4	-0.212	Very Coarse Sand
SORTING (σ):	4361.9	10.68	3.416	8.454	3.080	Very Poorly Sorted
SKEWNESS (Sk):	3.223	-1.603	1.603	-0.629	0.629	Very Fine Skewed
KURTOSIS (K):	14.99	4.711	4.711	1.935	1.935	Very Leptokurtic

SAMPLE STATISTICS

SAMPLE IDENTITY: **4553** UNIT **F3U3_a**
 SAMPLE TYPE: Unimodal, Poorly Sorted
 SEDIMENT NAME: Very Fine Sandy Coarse Silt

ANALYST & DATE: Adams, 16/01/2015
 TEXTURAL GROUP: Sandy Mud

	μm		ϕ		GRAIN SIZE DISTRIBUTION			
MODE 1:	23.44		5.500		GRAVEL: 0.0%		COARSE SAND: 0.0%	
MODE 2:					SAND: 13.2%		MEDIUM SAND: 0.0%	
MODE 3:					MUD: 86.8%		FINE SAND: 0.3%	
D ₁₀ :	2.258		3.752				V FINE SAND: 12.8%	
MEDIAN or D ₅₀ :	15.19		6.040		V COARSE GRAVEL: 0.0%		V COARSE SILT: 13.4%	
D ₉₀ :	74.21		8.791		COARSE GRAVEL: 0.0%		COARSE SILT: 22.6%	
(D ₉₀ / D ₁₀):	32.86		2.343		MEDIUM GRAVEL: 0.0%		MEDIUM SILT: 20.6%	
(D ₉₀ - D ₁₀):	71.95		5.038		FINE GRAVEL: 0.0%		FINE SILT: 14.2%	
(D ₇₅ / D ₂₅):	5.582		1.508		V FINE GRAVEL: 0.0%		V FINE SILT: 7.6%	
(D ₇₅ - D ₂₅):	27.78		2.481		V COARSE SAND: 0.0%		CLAY: 8.4%	
	METHOD OF MOMENTS				FOLK & WARD METHOD			
	Arithmetic	Geometric	Logarithmic		Geometric	Logarithmic	Description	
	μm	μm	ϕ		μm	ϕ		
MEAN (\bar{x}):	28.66	13.81	6.179		14.75	6.083	Medium Silt	
SORTING (σ):	44.72	3.516	1.814		3.713	1.893	Poorly Sorted	
SKEWNESS (Sk):	16.13	-0.345	0.345		-0.088	0.088	Symmetrical	
KURTOSIS (K):	484.3	2.653	2.653		1.032	1.032	Mesokurtic	

SAMPLE STATISTICS

SAMPLE IDENTITY: **4554** UNIT **F3U3_b**
 SAMPLE TYPE: Unimodal, Very Poorly Sorted
 SEDIMENT NAME: Muddy Very Fine Sand

ANALYST & DATE: Adams, 16/01/2015
 TEXTURAL GROUP: Muddy Sand

	μm		ϕ		GRAIN SIZE DISTRIBUTION		
MODE 1:	94.00		3.494		GRAVEL: 0.0%		COARSE SAND: 0.2%
MODE 2:					SAND: 68.5%		MEDIUM SAND: 0.2%
MODE 3:					MUD: 31.5%		FINE SAND: 1.2%
D ₁₀ :	1.652		3.119				V FINE SAND: 66.6%
MEDIAN or D ₅₀ :	76.22		3.714		V COARSE GRAVEL: 0.0%		V COARSE SILT: 4.1%
D ₉₀ :	115.1		9.241		COARSE GRAVEL: 0.0%		COARSE SILT: 2.2%
(D ₉₀ / D ₁₀):	69.64		2.963		MEDIUM GRAVEL: 0.0%		MEDIUM SILT: 4.4%
(D ₉₀ - D ₁₀):	113.4		6.122		FINE GRAVEL: 0.0%		FINE SILT: 3.9%
(D ₇₅ / D ₂₅):	6.454		1.805		V FINE GRAVEL: 0.0%		V FINE SILT: 5.6%
(D ₇₅ - D ₂₅):	83.33		2.690		V COARSE SAND: 0.3%		CLAY: 11.2%
	METHOD OF MOMENTS			FOLK & WARD METHOD			
	Arithmetic	Geometric	Logarithmic	Geometric	Logarithmic	Description	
	μm	μm	ϕ	μm	ϕ		
MEAN (\bar{x}):	75.48	34.70	4.849	30.78	5.022	Coarse Silt	
SORTING (σ):	96.36	5.198	2.378	4.975	2.315	Very Poorly Sorted	
SKEWNESS (Sk):	10.78	-1.283	1.283	-0.804	0.804	Very Fine Skewed	
KURTOSIS (K):	153.7	3.270	3.270	1.087	1.087	Mesokurtic	

SAMPLE STATISTICS

SAMPLE IDENTITY: 4557 UNIT F4U3
 SAMPLE TYPE: Bimodal, Poorly Sorted
 SEDIMENT NAME: Coarse Silt

ANALYST & DATE: Adams, 16/01/2015
 TEXTURAL GROUP: Mud

	μm		ϕ		GRAIN SIZE DISTRIBUTION			
MODE 1:	23.44		5.500		GRAVEL: 0.0%			COARSE SAND: 0.0%
MODE 2:	0.735		10.49		SAND: 0.9%			MEDIUM SAND: 0.0%
MODE 3:					MUD: 99.1%			FINE SAND: 0.0%
D ₁₀ :	1.533		4.840					V FINE SAND: 0.9%
MEDIAN or D ₅₀ :	12.98		6.268		V COARSE GRAVEL: 0.0%			V COARSE SILT: 10.8%
D ₉₀ :	34.91		9.350		COARSE GRAVEL: 0.0%			COARSE SILT: 31.8%
(D ₉₀ / D ₁₀):	22.78		1.932		MEDIUM GRAVEL: 0.0%			MEDIUM SILT: 24.0%
(D ₉₀ - D ₁₀):	33.38		4.510		FINE GRAVEL: 0.0%			FINE SILT: 12.1%
(D ₇₅ / D ₂₅):	4.580		1.405		V FINE GRAVEL: 0.0%			V FINE SILT: 8.3%
(D ₇₅ - D ₂₅):	18.30		2.195		V COARSE SAND: 0.0%			CLAY: 12.1%
		METHOD OF MOMENTS			FOLK & WARD METHOD			
	Arithmetic	Geometric	Logarithmic	Geometric	Logarithmic	Description		
	μm	μm	ϕ	μm	ϕ			
MEAN (\bar{x}):	17.30	9.975	6.647	10.01	6.642	Medium Silt		
SORTING (σ):	15.41	3.176	1.667	3.313	1.728	Poorly Sorted		
SKEWNESS (Sk):	2.032	-0.789	0.789	-0.340	0.340	Very Fine Skewed		
KURTOSIS (K):	12.60	2.885	2.885	1.085	1.085	Mesokurtic		

SAMPLE STATISTICS

SAMPLE IDENTITY: **4559** UNIT **F6U4**
 SAMPLE TYPE: Bimodal, Poorly Sorted
 SEDIMENT NAME: Coarse Silt

ANALYST & DATE: Adams, 16/01/2015
 TEXTURAL GROUP: Mud

	μm		ϕ		GRAIN SIZE DISTRIBUTION		
MODE 1:	23.44	5.500			GRAVEL: 0.0%		COARSE SAND: 0.0%
MODE 2:	0.735	10.49			SAND: 5.3%		MEDIUM SAND: 0.0%
MODE 3:					MUD: 94.7%		FINE SAND: 0.1%
D ₁₀ :	1.294	4.263					V FINE SAND: 5.1%
MEDIAN or D ₅₀ :	17.71	5.819			V COARSE GRAVEL: 0.0%		V COARSE SILT: 17.7%
D ₉₀ :	52.07	9.594			COARSE GRAVEL: 0.0%		COARSE SILT: 32.9%
(D ₉₀ / D ₁₀):	40.23	2.250			MEDIUM GRAVEL: 0.0%		MEDIUM SILT: 16.0%
(D ₉₀ - D ₁₀):	50.78	5.330			FINE GRAVEL: 0.0%		FINE SILT: 9.3%
(D ₇₅ / D ₂₅):	4.850	1.450			V FINE GRAVEL: 0.0%		V FINE SILT: 5.8%
(D ₇₅ - D ₂₅):	23.82	2.278			V COARSE SAND: 0.0%		CLAY: 13.1%
	METHOD OF MOMENTS			FOLK & WARD METHOD			
	Arithmetic	Geometric	Logarithmic	Geometric	Logarithmic	Description	
	μm	μm	ϕ	μm	ϕ		
MEAN (\bar{x}):	24.73	12.41	6.332	12.65	6.305	Medium Silt	
SORTING (σ):	40.88	3.709	1.891	3.845	1.943	Poorly Sorted	
SKEWNESS (Sk):	22.15	-0.791	0.791	-0.397	0.397	Very Fine Skewed	
KURTOSIS (K):	741.1	2.938	2.938	1.152	1.152	Leptokurtic	